Lappeenranta University of Technology
Faculty of Technology Management
Degree Program of Information Technology

Master's Thesis

Wei Liu

Development of Color Difference Equations Matching to Human Vision System

Examiners: Professor Heikki Kälviäinen
Docent, Dr.Tech. Arto Kaarna

ABSTRACT

Lappeenranta University of Technology
Faculty of Technology Management
Degree Program of Information Technology

Wei Liu

Development of Color Difference Equations Matching to Human Vision System

Master's thesis

2009

57 pages, 22 figures and 25 tables.

Examiners: Professor Heikki Kälviäinen
Docent, Dr. Tech. Arto Kaarna

Keywords: color spaces, color differences, color density, human vision system

Research on color difference evaluation has been active in recent thirty years. Several color difference formulas were developed for industrial applications. The aims of this thesis are to develop the color density which is denoted by g_{comb} and to propose the color density based chromaticity difference formulas. Color density is derived from the discrimination ellipse parameters and color positions in the xy, xyY and CIELAB color spaces, and the color based chromaticity difference formulas are compared with the line element formulas and CIE 2000 color difference formulas. As a result of the thesis, color density represents the perceived color difference accurately, and it could be used to characterize a color by the attribute of perceived color difference from this color.

PREFACE

This thesis was completed in the September, 2009, at the Machine Vision and Pattern Recognition Laboratory, Department of Information Technology of Lappeenranta University of Technology, Finland.

I would like to thank Professor Heikki Kälviäinen for offering me this opportunity to work on this thesis, and for his patient guidance and suggestions as well. I would also like to thank Docent, Dr.Tech. Arto Kaarna for his inspiring guidance, constructive help and discussions during this research.

Finally, I want to thank my parents and uncles for their care and support.

Wei Liu

September, 2009

TABLE OF CONTENTS

ABBREVIATIONS AND SYMBOLS

g_{ik}	Metric coefficient set
g_{11}	Metric coefficient
g_{12}	Metric coefficient
g_{22}	Metric coefficient
g_{comb}	Color density

BFD	BFD color difference formula
CIE	International Commission on Illumination
CIEDE00	The set of chromaticity discrimination ellipses for developing the CIEDE2000 color difference formula
CIEDE2000	CEIDE2000 color difference formula
CIELAB	CIE 1976 $La*b*$ color space
CIELUV	CIE 1976 $Lu*v*$ color space
CMC	CMC color difference formula
NCS	Natural Color System

1 INTRODUCTION

1.1 Background

Color difference evaluation is important in surface color industry and image processing. Several color difference formulas [1] have been developed to provide rather precious color difference evaluations for different application purposes. However, the computations of the color difference formulas are complicated and sophisticated, and causing different results for identical data [2] as well. Thus, the motivation for developing the color density is to provide an accurate way to estimate color differences with fewer computations.

1.2 Objectives and restrictions

The research questions of this work are forwarded as follows:

Research question 1: What is the mathematic form of color density?

Sub-question 1.1: What is the relationship between color density and color difference?

Sub-question 1.2: What is the mathematic form of the color density based color difference formula?

Research question 2: How to apply color density?

The color densities in the xy, xyY and CIELAB color spaces are developed from the metric coefficients g_{ik} [3] which can be calculated from the discrimination ellipses [3] and the color positions.

1.3 Structure of the thesis

This thesis consists of eight chapters: Chapter 1 gives an introduction. Chapter 2 discusses the structure of human eye and human color vision system. Chapter 3 presents basic definitions, attributes of color and the color spaces. Chapter 4 presents the forms for representing color difference data. Chapter 5 deals with developing the

color density and the color density based chromaticity difference formulas. Chapter 6 specifies the experiments. And the results are discussed in Chapter 7. In the end the conclusions are drawn in Chapter 8.

2 HUMAN VISION SYSTEM

It is well known that the visible light, whose wavelength is between 380 and 750 nm, is defined as different colors [3]. Color is perceived as a consequence of the interaction of illuminations, objects and the human vision system [4], as shown in Figure 1. Although color perception is highly subjective, the general mechanism and the mathematical model of observer vision system are of great importance in studying color measurement.

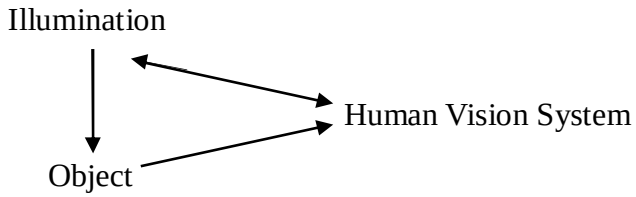

Figure 1. The interaction triangle of color [4].

2.1 Mechanism of human eyes

Images and colors are perceived by human eyes. A cross section of the structure of human eye is given in Figure 2, which illustrates its structure with some key features labeled. The human eye works like a camera: the cornea and the lens are cooperated like the camera lens to focus an object in the real world, and the image of the object are emerged on the retina at the back of the eye, which serves the same function as the image sensor of a camera [4]. The iris in the front of the eye defines the illumination level on the retina, which strongly influence the color perceived [4]; the ability of absorbing short-wavelength energy by the lens and the macula, which is known as yellow-filter effects, modulate the “spectral responsivity” [4] of human

vision system and introduce the “inter-observer variability” [4] in color perception. There are mainly two classes of photoreceptor cells in retina, rods and cones [3, 4], as shown in Figure 3. Rods mainly work at low luminance level (e.g., less than 1cd/m^2)

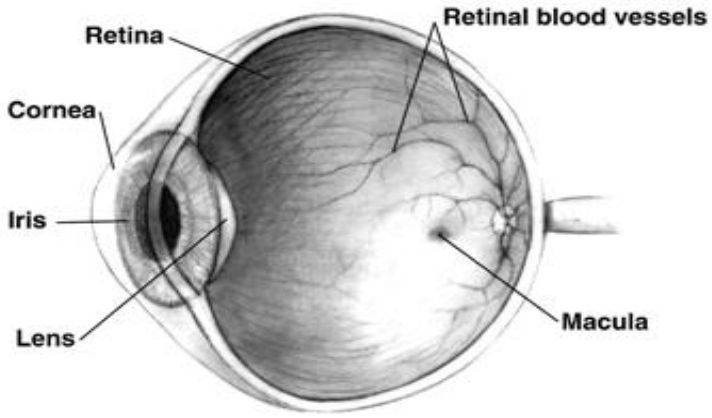

Figure 2. Human eye cross-sectional view [5].

and support black-white vision [3, 4]. In the contrary, cones mainly work at high luminance level (e.g., greater than 100 cd/m^2) and provide all the information to form human color sensation [3, 4]. There is only one type rod receptor responding to the peak spectrum at approximately 510 nm [4]. However, the three type cone receptors, which can be represented as L, M, and S cones, are able to respond through the whole visual spectrum [4], as shown in Figure 4.

The L, M, and S refer to the long-wavelength (500nm-700nm), middle-wavelength (450nm-630nm), and short-wavelength (400nm-500nm) sensitivity [4]. The cones also can be represented by R, G, and B cones, which refer to red sensitive, green sensitive and blue sensitive, respectively [4].

2.2 Mechanism of color vision

Trichromatic theory and opponent-colors theory are known as psychophysical models of color vision [3, 4]. These theories provided explanations of how the psychophysical outputs generated from the physical inputs of human vision system.

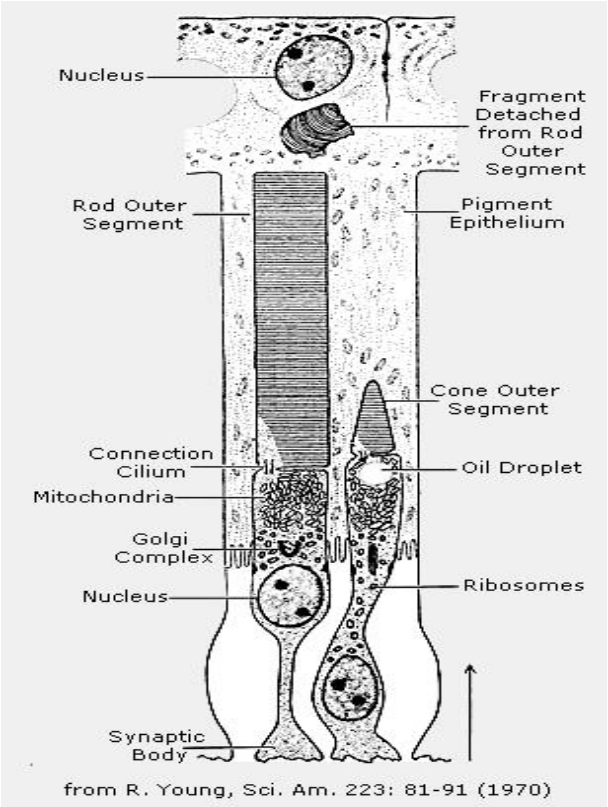

Figure 3. Rod cone cells [6].

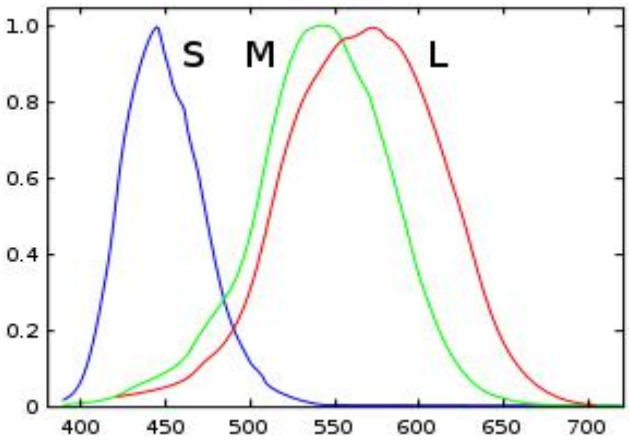

Figure 4. Spectral responsivities of L, M, and S cones [7].

Trichromatic theory proposed that color vision was a result of three types of cone cells, which were sensitive to the red, green and blue respectively. Three kind cone signals of each real world image were transmitted to the brain where the signals were correlated in a direct and simple way to generate the color vision [3, 4].

Component-colors theory stated the visual process was interactions between opposite pairs of signals, and the three pairs of signals were light-dark, red-green and yellow-blue. The cells of retina encoded the color into the opponent signals [4]. Compared with trichromatic theory, the opponent-colors theory explained the color stimuli appearance or color perception more accurately and efficiently [3].

2.3 Human visual response

The quantitative responsivities of human vision system can be represented by color matching functions between two color stimuli [3, 4] as

$$\int_{\lambda} P_1(\lambda)\, L(\lambda)\, d\lambda = \int_{\lambda} P_2(\lambda)\, L(\lambda)\, d\lambda\,, \tag{1}$$

$$\int_{\lambda} P_1(\lambda)\, M(\lambda)\, d\lambda = \int_{\lambda} P_2(\lambda)\, M(\lambda)\, d\lambda\,, \tag{2}$$

and

$$\int_{\lambda} P_1(\lambda)\, S(\lambda)\, d\lambda = \int_{\lambda} P_2(\lambda)\, S(\lambda)\, d\lambda\,, \tag{3}$$

where $P_1(\lambda)$ and $P_2(\lambda)$ are the spectral power distributions of two stimuli, and $L(\lambda)$, $M(\lambda)$, and $S(\lambda)$ represent the three cone responsivities. Only three integrations are needed for color matching, so $P_1(\lambda)$ and $P_2(\lambda)$ are not have to be equal for every wavelength [4].

3 COLOR AND COLOR SPACES

To discuss the measurement of color differences or the relatively magnitude between two color stimuli, several fundamental attributes of color should first be understood: Color spaces show the geometrical models of human color perceptions [8]. Color also can be represented by tristimulus values [3] or other quantitative attributes in different color spaces.

3.1 Fundamental attributes of color perceptions

Perceptual color can be defined in a non-quantitative manner. Table 1 gives some fundamental attributes of perceptual color.

Table 1. Fundamental attributes of color perceptions [3, 4].

Hue	Hue is an attributes of a visual sensation which can be described as red, yellow, blue, green, purple, and so on. A chromatic color is perceived with hue. An achromatic color is perceived devoid of hue.
Lightness	Lightness reflects the color stimulus which emits more or less light under a certain illumination and view condition.
Chroma	Chroma defines the degree to which a chromatic color stimulus differs from an achromatic color stimulus.

3.2 Tristimulus values and chromaticity diagram

The relationship between a color stimulus and a set of color primaries [4] is given as

$$C \equiv R\,(\boldsymbol{R}) + G\,(\boldsymbol{G}) + B\,(\boldsymbol{B}), \qquad (4)$$

where C is the specific color stimulus, the script terms $\boldsymbol{R}\ \boldsymbol{G}\ \boldsymbol{B}$, are primaries which are defined by different primary sets, and $R, G,$ and B are known as the tristimulus values, which indicate the amount of the primaries needed to specify the given color stimulus. Therefore, Eq.4 indicates that the color C is represented by R units of primary $\boldsymbol{R}$, G units of primary $\boldsymbol{G}$, and B units of primary $\boldsymbol{B}$ [4].

There are two sets of tristimulus values, the $R\ G\ B$ tristimulus values and the $X\ Y\ Z$ tristimulus values [4]. However, the $X\ Y\ Z$ tristimulus value set overcomes negative amount of primary which might be needed in representing a color by the $R\ G\ B$ tristimulus value set. The way to calculate the $X\ Y\ Z$ tristimulus values is illustrated as

$$X = k \int_{\lambda} P(\lambda)\,\bar{x}(\lambda)\,d\lambda, \tag{5}$$

$$Y = k \int_{\lambda} P(\lambda)\,\bar{y}(\lambda)\,d\lambda, \tag{6}$$

$$Z = k \int_{\lambda} P(\lambda)\,\bar{z}(\lambda)\,d\lambda, \tag{7}$$

$$k = \frac{100}{\int_{\lambda} S(\lambda)\bar{y}(\lambda)d\lambda}, \tag{8}$$

where $P(\lambda)$ indicates the spectral power distribution, $\bar{x}(\lambda), \bar{y}(\lambda)$ and $\bar{z}(\lambda)$ are the CIE 1931 *2*° color matching functions, $S(\lambda)$ is the "spectral concentration of the radiant power of the source illuminating the object" [3].

The chromaticity diagram was developed to provide a two-dimensional representation of colors. The transformation from the tristimulus values to chramaticity diagrams is given by:

$$x = \frac{X}{X+Y+Z}, \tag{9}$$

$$y = \frac{Y}{X+Y+Z}, \tag{10}$$

$$z = \frac{Z}{X+Y+Z}. \tag{11}$$

Since chromaticity diagram tries to specify a color stimulus by two-dimensional information x and y, the third dimensional information z can always be obtained from

$$z = 1 - x - y . \tag{12}$$

3.3 CIE color space

CIELUV and CIELAB are the two color spaces recommended by CIE. These spaces have three-dimensional coordinates which approximately relate the tristimulus values with the perceived lightness, chroma, and hue for a color stimulus. However, the main purpose for developing these color space is to promote the uniformity of color difference formulas [4].

The CIELUV color space is defined by

$$L^* = 116\left(\frac{Y}{Y_n}\right)^{1/3} - 16, \tag{13}$$

$$u^* = 13L^*\left(u' - u_n'\right), \tag{14}$$

$$v^* = 13L^*\left(v' - v_n'\right), \tag{15}$$

with

$$u' = \frac{4X}{X + 15Y + 3Z} \qquad v' = \frac{9Y}{X + 15Y + 3Z}, \tag{16}$$

$$u_n' = \frac{4X_n}{X_n + 15Y_n + 3Z_n} \qquad v_n' = \frac{9Y_n}{X_n + 15Y_n + 3Z_n}. \tag{17}$$

Similarly, the CIELAB color space is defined as

$$L^* = 116\left(\frac{Y}{Y_n}\right)^{1/3} - 16, \tag{18}$$

or

$$L_m^* = 903.3\frac{Y}{Y_n} \qquad \text{for } \frac{Y}{Y_n} \le 0.008856, \tag{19}$$

and

$$a^* = 500\left[f\left(\frac{X}{X_n}\right) - f\left(\frac{Y}{Y_n}\right)\right], \tag{20}$$

$$b^* = 200\left[f\left(\frac{Y}{Y_n}\right) - f\left(\frac{Z}{Z_n}\right)\right], \tag{21}$$

where

$$\mathrm{f}(\omega) = (\omega)^{1/3} \qquad \omega > 0.008856, \tag{22}$$

or

$$\mathrm{f}(\omega) = 7.787(\omega) + 16/116 \qquad \omega \le 0.008856. \tag{23}$$

In Eqs. 13 to 23, $X\ Y\ Z$ are the tristimulus values of the stimulus and $X_n\ Y_n\ Z_n$ are the tristimulus values of the reference white.

Figure 5 illustrates cylindrical representation of the CIELAB color space, L^* measures the perceived lightness which is ranging from black (0.0) to white (100.0), a^* indicates the red-green chroma perceptions and b^* indicates the yellow-blue chroma perceptions. In addition, cylindrical representation of the CIELAB color space provides the ways for calculating chroma C_{ab}^* and hue angle in degrees h_{ab}:

$$C_{ab}^* = \sqrt{\left(a^{*2} + b^{*2}\right)}, \tag{24}$$

$$h_{ab} = \tan^{-1}\left(\frac{b^*}{a^*}\right), \tag{25}$$

The lightness definition L^* for the CIELUV color space is identical to the CIELAB color space, but there are no simple relationships between a^* b^* in CIELAB and

$u^* v^*$ in CIELUV. As compared to CIELUV, CIELAB is more popular used for color difference measurement [3, 4].

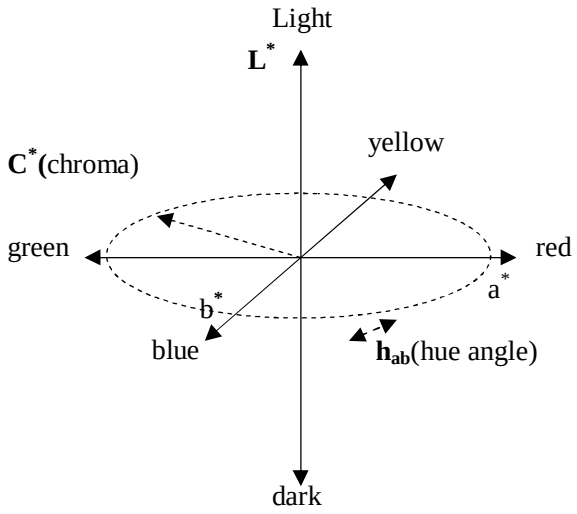

Figure 5. Cylindrical representation of the CIELAB color space [4].

3.4 Munsell color system and Natural color system (NCS)

The Munsell color system [9, 10] and Natural color system (NCS) [11] are color spaces which arrange color chips in three dimensions. The color chips [12] used in these color space represent the human color sensation. In the case of Munsell color system, color chips are ordered in terms of three attributes: hue, value (lightness), and chroma. In the case of NCS, the space contains blackness, whiteness, hue, and chromatiness.

The major differences in structure between these two color spaces may be mentioned here. First, the NCS is not equally visually spaced, the NCS chromatiness is always set with respect to the hue value [13, 14]. Second, the lightness attributes in the Munsell color system are not specified explicitly in NCS [13, 14].

4 COLOR DIFFERENCES

The line elements [1, 15], which are denoted as ds or ΔE, are developed as mathematical formulations to measure the color discriminations. Color discrimination data are mostly represented in the form of discrimination ellipses in chromaticity diagram or in color spaces. Color discrimination data can be calculated from color difference formulas, and each color difference formula is developed for specific application purpose.

4.1 Line elements in color space

From a geometric point of view, a line element is a measured distance in a color space, and the perceived color difference can be characterized by the line element. Therefore, line elements are mostly used for identifying pairs of color stimuli which present a particular constant color difference [3].

Supposed that (U_1, U_2, U_3) and $(U_1 + dU_1, U_2 + dU_2, U_3 + dU_3)$ represent a pair of color stimuli in a color space, the line element between them is defined as [3]

$$\Delta E = \sqrt{g_{11}(dU_1)^2 + 2g_{12}dU_1dU_2 + g_{22}(dU_2)^2 + 2g_{23}dU_2dU_3 + g_{33}(dU_3)^2 + 2g_{31}dU_3dU_1} \tag{26}$$

where the metric coefficients g_{ik} can be continuous functions of the color space coordinates. Then, a suitably calculated line element is the just-noticeable color difference for this pair.

4.2 Discrimination ellipses

4.2.1 MacAdam ellipse set

MacAdam ellipses [16, 17] are known as the chromaticity difference ellipses, which

measure the color differences perceived by human vision system in the *xy* chromaticity diagram. The area inside each ellipse represents the same perceived color differences, in other words, the chromaticity differences inside the ellipse can not be perceived. There are 25 MacAdam ellipses in total as shown in Figure 6.

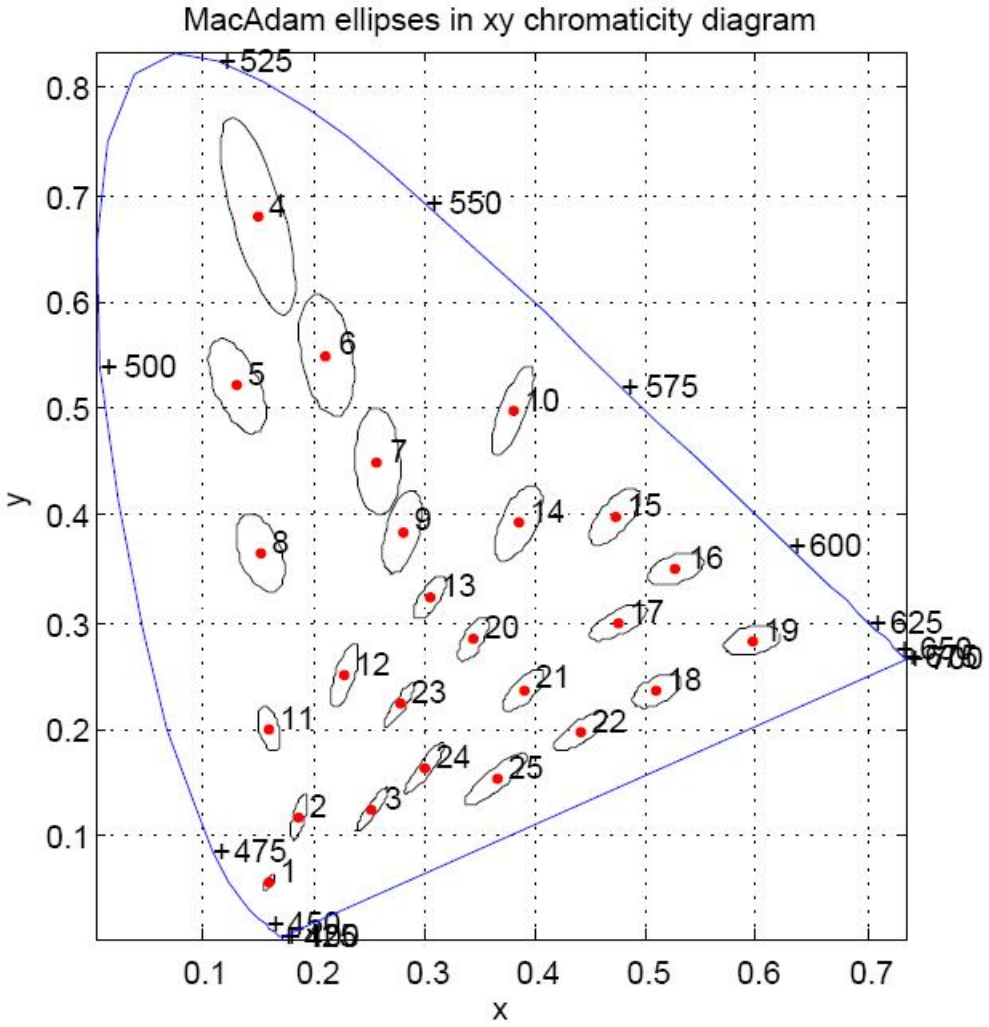

Figure 6. MacAdam ellpses in the *xy* chromaticity diagram, each ellipse is drawn to ten times its real size in relation to the coordinate scale.

Each of the twenty-five ellipses can be defined as

$$g_{11}dx^2 + 2g_{12}dxdy + g_{22}dy^2 = 1, \tag{27}$$

where dx is the difference of x coordinates between the ellipse center and any

point on the ellipse, dy is the difference of y coordinates for the same pair of points [3, 17], and the metric coefficients g_{ik} are constant for each ellipse.

The values of g_{11}, g_{12} and g_{22} can be computed from the length of major semi-axes a, the length of minor semi-axes b of each ellipse, and the inclination angle θ of the major semi-axes to the axis of x coordinates [17]. The computing processes are shown as

$$g_{11} = \cos^2\theta / a^2 + \sin^2\theta / b^2, \tag{28}$$

$$g_{12} = \sin\theta\cos\theta(1/a^2 - 1/b^2), \tag{29}$$

$$g_{22} = \sin^2\theta / a^2 + \cos^2\theta / b^2. \tag{30}$$

The size, shapes and orientations of ellipses vary systematically over the diagram, for example, the ellipses at the bottom left corner, which is the blue area, are the smallest, and the angles of inclination are also the smallest. Both the size and inclination angles become larger from the bottom to the top gradually, and reach the maximum at the top left corner, which is the green area.

4.2.2 CIEDE00 discrimination ellipses set

Four original ellipse datasets, RIT-DuPont, Witt, Leeds and BFD-P, are combined and adjusted into a new consistent dataset [18]. This new dataset was used for developing the CIEDE2000 color difference formula [19], which is denoted as CIEDE00 discrimination ellipses set in this work. Figure 7 shows the CIEDE00 ellipse dataset in the a^*b^* diagram.

Some clear trends can be seen from Figure 7: ellipses close to the grey axis (around a* between -10 and 10, b* between -15 and 15) are the smallest, ellipse size increases

as chromaticity increase, and nearly all ellipses point towards the grey axis except for those in blue area (particularly around a*= 10, b*= -40) [19].

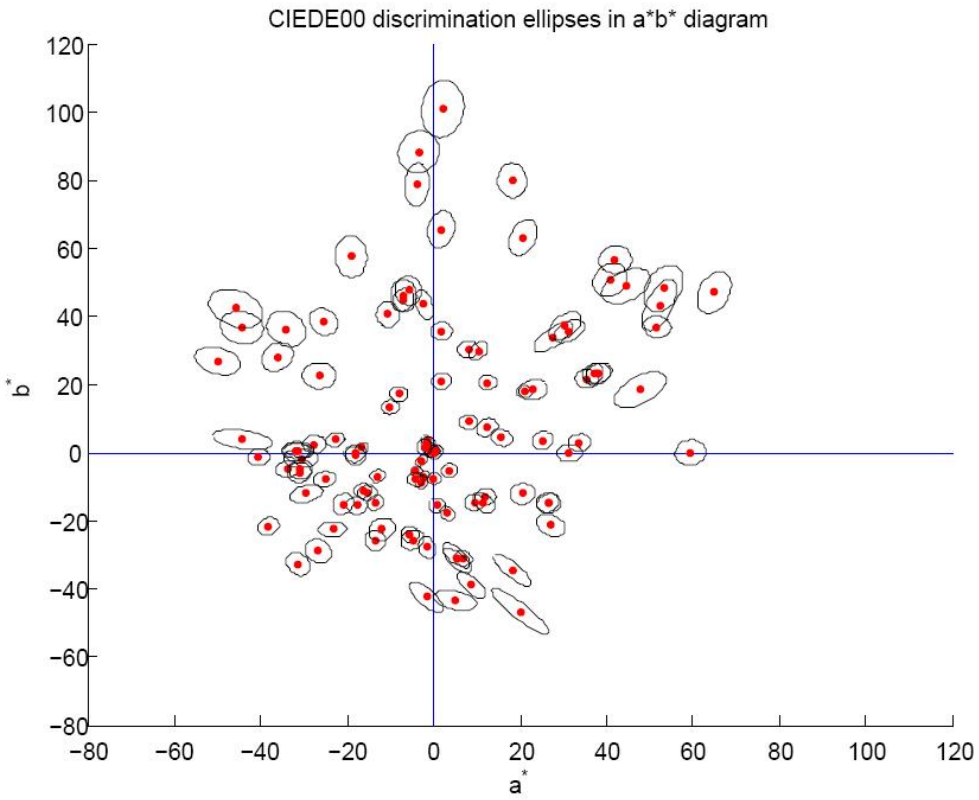

Figure 7. CIEDE00 discrimination ellipses plotted in the a*b* diagram.

4.3 CIELAB-based color differences formulas

The original color difference formula associated with CIELAB color space is:

$$\Delta E^*_{ab} = \left[\left(\Delta L^*\right)^2 + \left(\Delta a^*\right)^2 + \left(\Delta b^*\right)^2 \right]^{1/2}, \tag{31}$$

where $\Delta L^*, \Delta a^*$ and Δb^* are differences in terms of L^*, a^* and b^* [20].

However, Eq. 31 is too limited with the different industrial application purpose. Consequently, several advanced color difference formulas based on CIELAB were developed, which are known as the CMC [21], BFD [22, 23], CIE94 [24, 25] and CIE2000 color difference formula. The CMC color difference formula has been

standardized within the textile industry [21, 20]. The BFD color difference formula also has been used by industry application successfully [22]. Although the CIE94 color difference formula is similar with the CMC color difference formula, it is a mathematically simpler equation with significantly improving the prediction of perceptible color differences [22]. The newest color difference formula, denoted as CIEDE2000 color difference formula, outperformed the CMC and CIE94 formulas by a large margin, and predicted better than the BFD formula [20].

The common structure [26, 20] for these advanced color difference formulas is shown as

$$\Delta E^* = \left[\left(\frac{\Delta L^*}{k_L S_L} \right)^2 + \left(\frac{\Delta C^*}{k_C S_C} \right)^2 + \left(\frac{\Delta H^*}{k_H S_H} \right)^2 + \Delta R \right]^{1/2}, \tag{32}$$

with

$$\Delta R = R_T \, f\left(\Delta C^* \Delta H^*\right), \tag{33}$$

where $\Delta L^*, \Delta C^*$ and ΔH^* are lightness, chroma, and hue differences which can always be computed from the CIELAB color space, k_L, k_C, and k_H are the parametric factors to be adjusted for different experimental conditions for lightness, chroma, and hue components, S_C, S_L, and S_H are the weighting functions for keeping the perceptual uniformity of the CIELAB color space, ΔR is used for rotating the chromatic ellipses in blue regions of the a^*b^* diagram. However, ΔR is always set to be zero for the CMC and CIE94 color difference formulas [21, 22, 26].

5 DENSITY OF COLORS

Considering that color density could indicate the perceived color differences which were defined in Eq. 26, thus color density could be derived from the metric coefficients g_{ik} in the xy chromaticity diagram, *xyY* color space and CIELAB color space.

5.1 Density of colors in the xy chromaticity diagram

For developing the color density in the xy chromaticity diagram, two new g-values $g_{\max}$ and $g_{\min}$ which are coefficients along the major semi-axes a and minor semi-axes b of the ellipse should be calculated firstly. The computations of $g_{\max}$ and $g_{\min}$ are based on the von Mises yield criterion [27] in material science. The $g_{\max}$ and $g_{\min}$ could be calculated from

$$g_{\max} = \frac{g_{11} + g_{22}}{2} + \sqrt{\left(\frac{g_{11} - g_{22}}{2}\right)^2 + {g_{12}}^2}, \tag{34}$$

and

$$g_{\min} = \frac{g_{11} + g_{22}}{2} - \sqrt{\left(\frac{g_{11} - g_{22}}{2}\right)^2 + {g_{12}}^2}. \tag{35}$$

The values of g_{11}, g_{12} and g_{22} can be calculated from the MacAdam ellipses parameters, as given in Eqs. 28, 29 and 30.

Then the $g_{\max}$ and $g_{\min}$ in two directions could be combined to a single value g_{comb}, and this value is developed as the color density. Thus the color density g_{comb} is defined as

$$g_{comb} = \sqrt{{g_{\max}}^2 - g_{\max} g_{\min} + {g_{\min}}^2}. \tag{36}$$

However, in order to develop the density for all the colors in the xy chromaticity diagram, the values of g_{11}, g_{12} and g_{22} should be interpolated over the entire

chromaticity diagram.

5.2 Density of colors in the CIELAB color space

The perceived chromaticity differences of human vision system in the CIELAB space are represented by CIEDE00 ellipses set. However, the illumination level is a constant for each individual ellipse, in other words, the illumination differences equal to zero for each ellipse. Thus, the same method and equations could be used for developing the color density in CIELAB as in the *xy* chromaticity diagram. The color density in the CIELAB space would also be denoted by g_{comb}.

5.3 Density of colors in the *xyY* color space

The *xyY* color space can be seen as an extension of the *xy* chromaticity diagram, while the *Y* coordinate indicates the illumination levels. Given that the illumination factor also influences the perceived color differences, therefore, the g_{11}, g_{12} and g_{22} values in the *xyY* color space [28] are computed from the processes as follows.

In the CIELAB color space, the chromaticity difference ΔC (ΔY =0) is defined as

$$\Delta C = \sqrt{(\Delta a^*)^2 + (\Delta b^*)^2}\ . \tag{37}$$

Since the chromaticity position in a^*b^* diagram can be calculated by:

$$a^* = 500[(\frac{X}{X_n})^{\frac{1}{3}} - (\frac{Y}{Y_n})^{\frac{1}{3}}], \tag{38}$$

$$b^* = 200[(\frac{Y}{Y_n})^{\frac{1}{3}} - (\frac{Z}{Z_n})^{\frac{1}{3}}], \tag{39}$$

where $X = (\frac{x}{y})Y$, $Z = (\frac{z}{y})Y$ and $z = 1 - x - y$; and the reference white in this

calculation is X_n =94.811, Y_n =100.00 and Z_n =107.304,

the partial derivatives are calculated as

$$a_x = \frac{\partial a^*}{\partial x} = 500(\frac{Y}{X_n})^{\frac{1}{3}} 500(\frac{Y}{Y_n})^{\frac{1}{3}} \frac{1}{3}(\frac{x}{y})^{-\frac{2}{3}}(\frac{1}{y}), \tag{40}$$

$$a_y = \frac{\partial a^*}{\partial y} = 500(\frac{Y}{X_n})^{\frac{1}{3}} 500(\frac{Y}{Y_n})^{\frac{1}{3}} \frac{1}{3}(\frac{x}{y})^{-\frac{2}{3}}(-\frac{x}{y^2}), \tag{41}$$

$$b_x = \frac{\partial b^*}{\partial x} = -200(\frac{Y}{Z_n})^{\frac{1}{3}} 200(\frac{Y}{Y_n})^{\frac{1}{3}} \frac{1}{3}(\frac{z}{y})^{-\frac{2}{3}}(-\frac{1}{y}), \tag{42}$$

$$b_y = \frac{\partial b^*}{\partial y} = -200(\frac{Y}{Z_n})^{\frac{1}{3}} 200(\frac{Y}{Y_n})^{\frac{1}{3}} \frac{1}{3}(\frac{z}{y})^{-\frac{2}{3}}(\frac{-y-z}{y^2}). \tag{43}$$

Thus the Eq.37 could be represented as

$$\Delta C = \sqrt{(a_x^{\ 2} + b_x^{\ 2})(dx)^2 + 2(a_x a_y + b_x b_y)dxdy + (a_y^{\ 2} + b_y^{\ 2})(dy)^2}\ . \tag{44}$$

However, for each individual ellipse in the CIEDE00 ellipses set, dY =0, thus Eq. 26 could be simplified as:

$$\Delta E = \sqrt{g_{11}(dx)^2 + 2g_{12}dxdy + g_{22}(dy)^2}\ , \tag{45}$$

where

$$g_{11} = a_x^{\ 2} + b_x^{\ 2}, \tag{46}$$

$$g_{12} = a_x a_y + b_x b_y, \tag{47}$$

$$g_{22} = a_y^{\ 2} + b_y^{\ 2}. \tag{48}$$

The $g_{\max}$, $g_{\min}$ and g_{comb} values could be computed from Eqs. 34, 35 and 36.

5.4 Computing chromaticity differences from color density

For examining the perceived color differences which are estimated by color density, a set of color density-based chromaticity difference formulas are proposed in this work.

As illustrated in Fig. 8, let (x_0, y_0) and (x_i, y_i) denote chromaticity C1 and chromaticity C2, and (x_0, y_0) is the starting point.

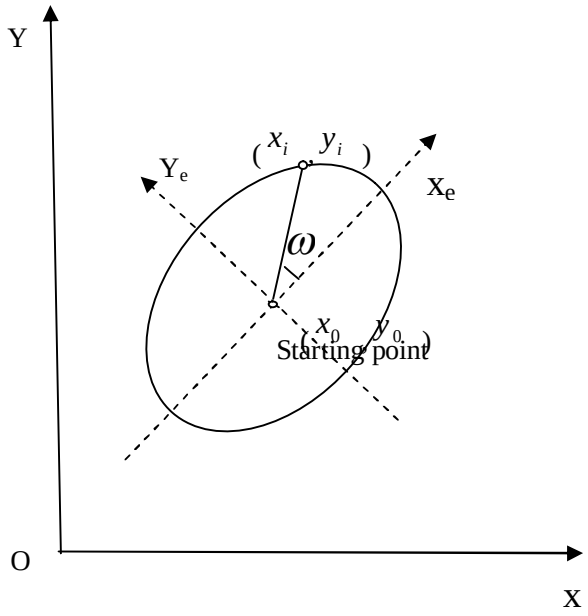

Figure 8. The visualization of the chromaticity points.

The Euclidean distance dis between C1 and C2 is defined as

$$dis = \sqrt{dx^2 + dy^2}\,, \tag{49}$$

with $dx = x_0 - x_i$, $dy = y_0 - y_i$.

The chromaticity differences between C1 and C2 are calculated by

$$ds1 = \sqrt{g_{11}dx^2 + 2g_{12}dxdy + g_{22}dy^2}\,, \tag{50}$$

and

$$ds2 = \sqrt{g_{11i}dx^2 + 2g_{12i}dxdy + g_{22i}dy^2}\,. \tag{51}$$

The color density-based chromaticity differences between C1 and C2 are defined as

$$ds3 = \sqrt{g_{\max i}dx_e^{\ 2} + g_{\min i}dy_e^{\ 2}}\,, \tag{52}$$

$$ds4\_1 = \sqrt{g_{combi}dx^2 + g_{combi}dy^2}\,, \tag{53}$$

and

$$ds4\_2 = g_{comi} dis\,, \tag{54}$$

where g_{11}, g_{12} and g_{22} are the metric coefficients of the starting point C1, g_{11i}, g_{12i} and g_{22i} are the mean values of the interpolated g_{ij} values of C1 and C2, and g_{combi} are the mean values of the interpolated g_{comb} values of C1 and C2. dx_e and dy_e are the differences of X_e and Y_e coordinates.

6 EXPERIMENTS

For each ellipse in the xy chromaticity diagram, xyY color space and CIELAB color space, the g_{comb} values were computed, and then the chromaticity differences defined in Eqs.49 to 54 are calculated from the ellipse center to the selected chromaticity points related to each ellipse. In particular, the chromaticity differences were computed by the CIEDE2000, CIE94 and CMC color difference formulas in CIELAB, as well.

6.1 Interpolation

As discussed in Chapter 4, the variation trends of the MacAdam ellipses were systematical. These trends encourage the interpolation of ellipses throughout the xy chromaticity diagram. The ellipses also can be constructed from the g_{ik} values by

$$\tan 2\theta = 2g_{12}/(g_{11} - g_{22}) \qquad \theta < 90^\circ \text{ when } g_{12} < 0,\ \theta > 90^\circ \text{ when } g_{12} > 0, \tag{55}$$

$$1/a^2 = g_{22} + g_{12}\cot\theta, \tag{56}$$

$$1/b^2 = g_{11} - g_{12}\cot\theta. \tag{57}$$

where θ, a and b are the ellipses parameters.

With the help of the original study of the MacAdam ellipses [17], the g_{ik} values along the color gamut could be estimated. Both computed and estimated values are used for interpolation. Therefore in every location in the chromaticity diagram, the g_{comb} value could be computed.

However, for the xyY and CIELAB color spaces, the CIEDE00 ellipse sets were the only available information. For this reason, the interpolations could be performed

only inside the areas which were enclosed by CIEDE00 ellipse sets. The BFD-P, Rit-DuPont and Witt data sets which are 116 ellipses in total were used for interpolation in this work.

The interpolation of g_{ik} values in Matlab environment was made by using the linear interpolation method, as well as the nearest-neighbor interpolation method. The later could avoid the null values which might caused by the former.

6.2 Designed experiments

In each experiment, four pairs of chromaticity points were fixed for each ellipse, and then the color differences and Euclidean distance are computed.

6.2.1 Experiment 1

The first experiment was performed between the ellipse center and the chromaticity points on each ellipse boundary, and the fixed chromaticity points are shown in Figure 9.

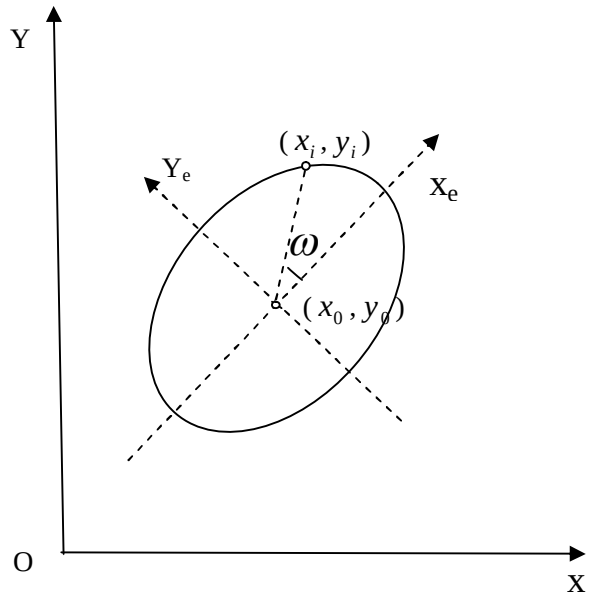

Figure 9. Fixed chromaticity points along a discrimination ellipse boundary.

6.2.2 Experiment 2

The second experiment was performed for circles, the ellipse centers are taken as the circle centers, and the lengths of radii of circles r are the lengths of ellipse major semi-axes a. Thus, the sizes of circles vary in various locations. The fixed chromaticity points are shown in Figure 10.

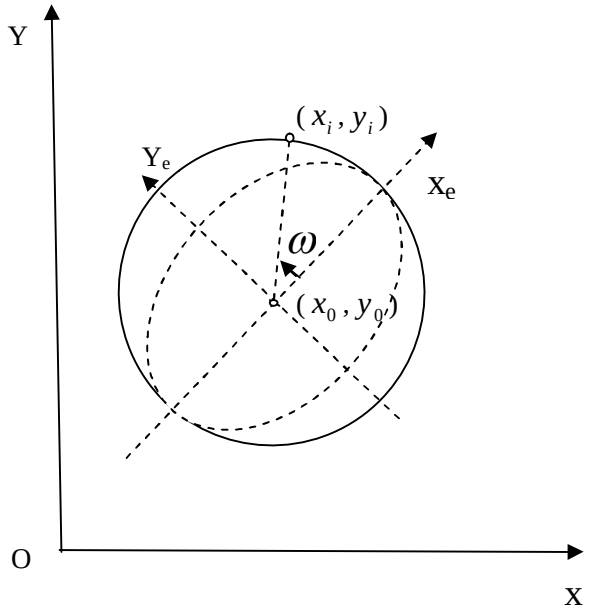

Figure 10. Fixed chromaticity points along a circle, the radii of the circle $r = a$.

6.2.3 Experiment 3

The third experiment was also performed for circles. The ellipse centers are taken as the circle centers, and the lengths of radii of circles r are constant everywhere. The constant radii r are the set of the mean values of the ellipse major semi-axes a, which are 0.0034 in xy chromaticity diagram, 0.0087 in xyY color space and 2.28 in CIELAB, respectively. The fixed chromaticity points are shown in Figure 11.

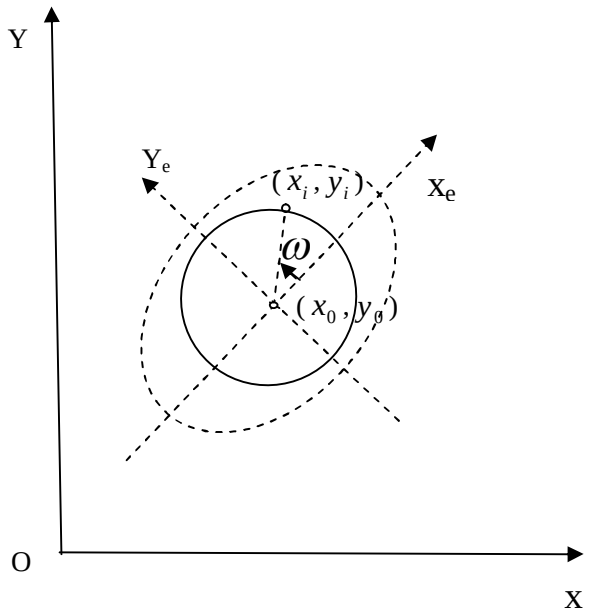

Figure 11. Fixed chromaticity points along a circle with constant radius r.

6.3 Experimental results

6.3.1 Experimental results of interpolation

New g_{11}, $2\,g_{12}$ and g_{22} data on or near the color gamut were estimated for interpolation in *xy* chromaticity diagram. Tables 2-4 collect the estimated data. Each of Figures 12-14 illustrateed the interpolated g_{11}, $2\,g_{12}$ and g_{22} throughout the chromaticity diagram, respectively. In Figure 15, the new ellipses were plotted at the different locations which cover different color areas, and the original MacAdam ellipses were plotted in red, and new ellipses plotted in blue were constructed from the interpolated g_{11}, g_{12} and g_{22} data. All the ellipses were enlarged 10 times to their original sizes.

Figure 16 and 17 present the ellipses which were constructed from the interpolated g_{11}, g_{12} and g_{22} data in the *xyY* color space and CIELAB color space, respectively. In these two figures, the five original CIE discrimination ellipses are

plotted in red, and the blue ellipses were plotted from the interpolated g_{ik} value.

Table 2. The estimated g_{11} values on the color gamut in the *xy* chromaticity diagram.

x	y	g_{11}
0.075	0.200	80.000
0.125	0.060	430.000
0.160	0.020	800.000
0.350	0.080	96.000
0.480	0.130	29.400
0.330	0.330	31.000
0.280	0.700	42.000
0.700	0.250	10.500
0.670	0.350	12.000
0.450	0.550	75.000

Table 3.The estimated $2\,g_{12}$ values on the color gamut in the *xy* chromaticity diagram.

x	y	$2\,g_{12}$
0.210	0.010	-616.00
0.320	0.070	-343.000
0.370	0.100	-122.200
0.280	0.720	-20.000
0.070	0.030	3.400
0.101	0.075	15.000
0.280	0.700	30.000
0.040	0.320	40.000
0.060	0.245	50.000
0.097	0.116	70.000

Table 4. The estimated g_{22} values on the color gamut in the *xy* chromaticity diagram.

x	y	g_{22}
0.180	0.020	370.000
0.230	0.040	252.000
0.710	0.275	110.400
0.630	0.360	55.000
0.040	0.440	21.500
0.015	0.500	13.800
0.300	0.700	10.000
0.005	0.600	6.000
0.015	0.745	3.660
0.020	0.800	1.368

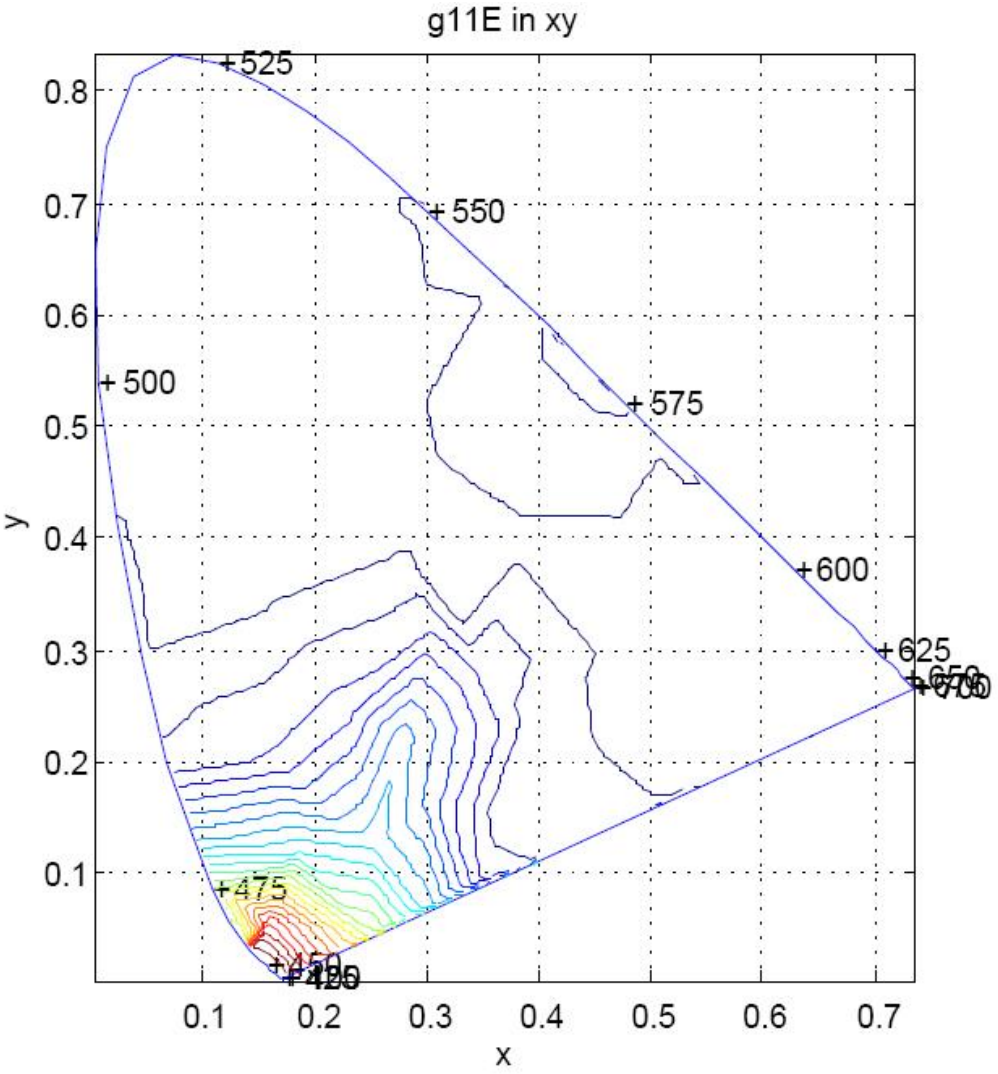

Figure 12. Contours of coefficient g_{11} in the xy diagram.

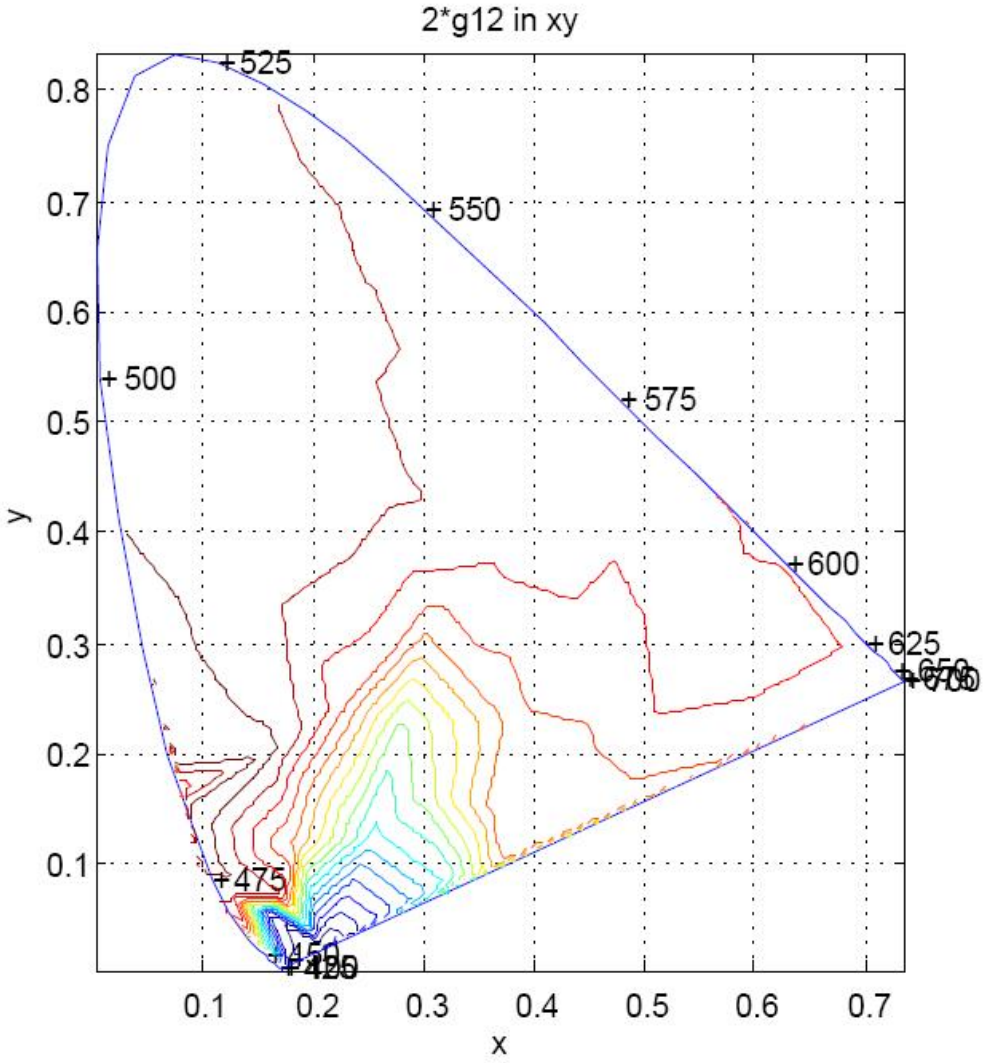

Figure 13. Contours of coefficient $2\,g_{12}$ in the xy diagram.

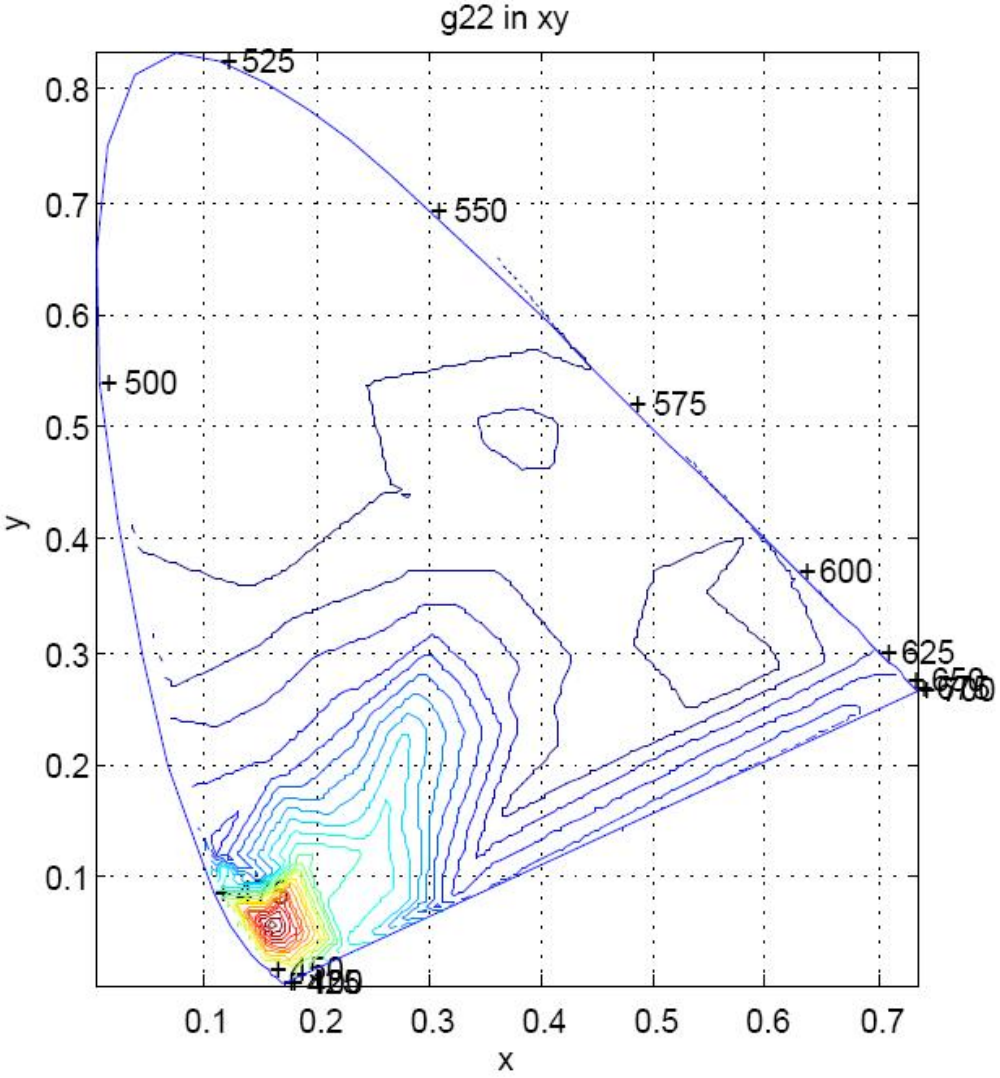

Figure 14. Contours of coefficient g_{22} in the xy diagram.

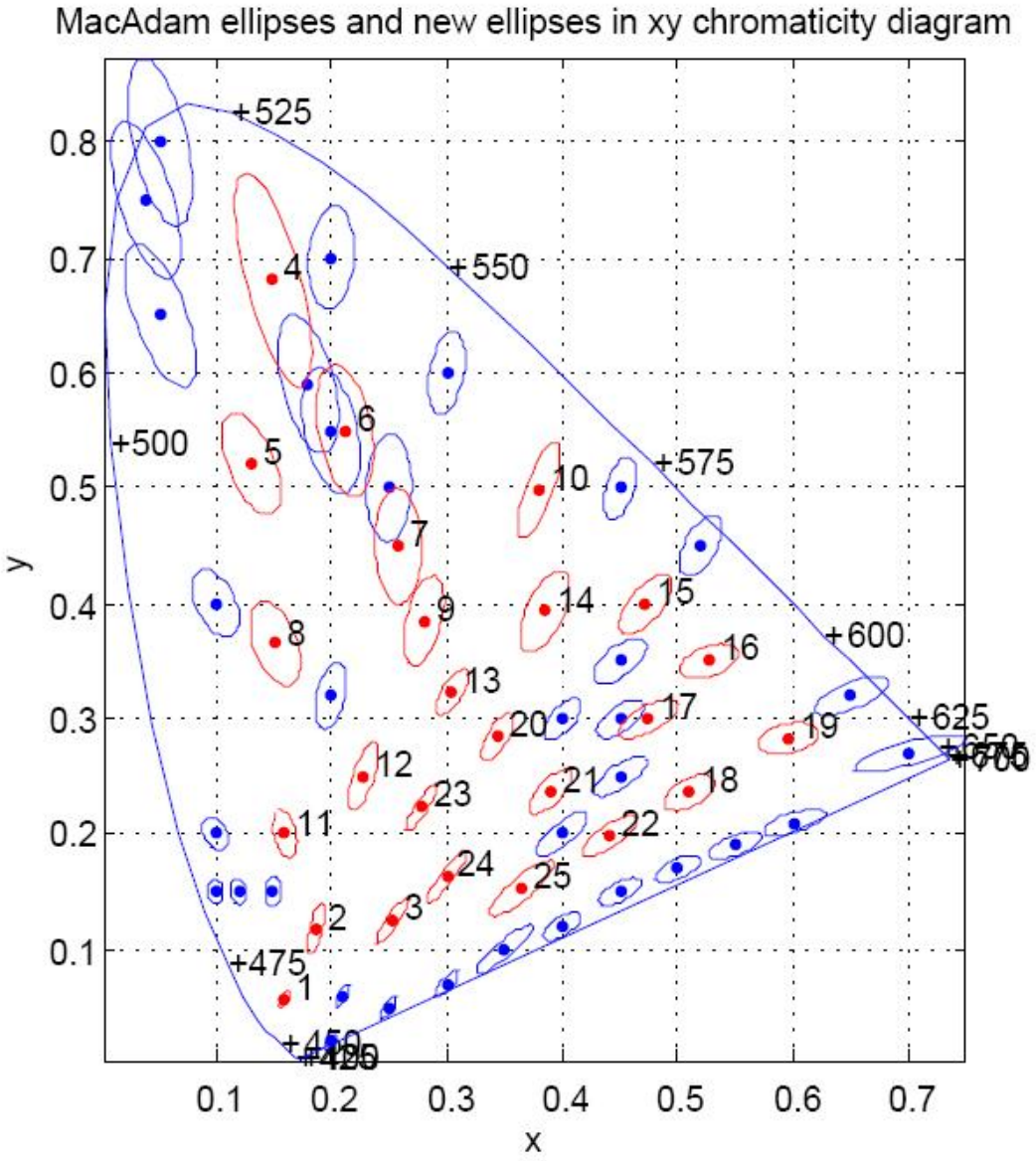

Figure 15. The original MacAdam Ellipses (red set) and new chromaticity ellipses (blue set)

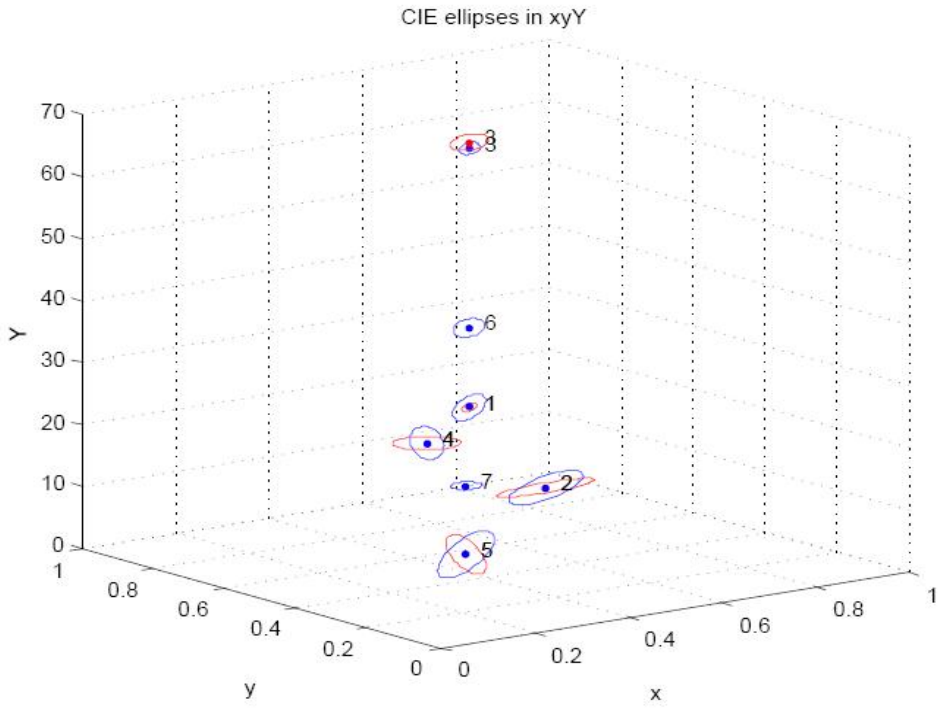

Figure 16. CIE chromaticity ellipses (red set) and new ellipses (blue set) in the *xyY* color space.

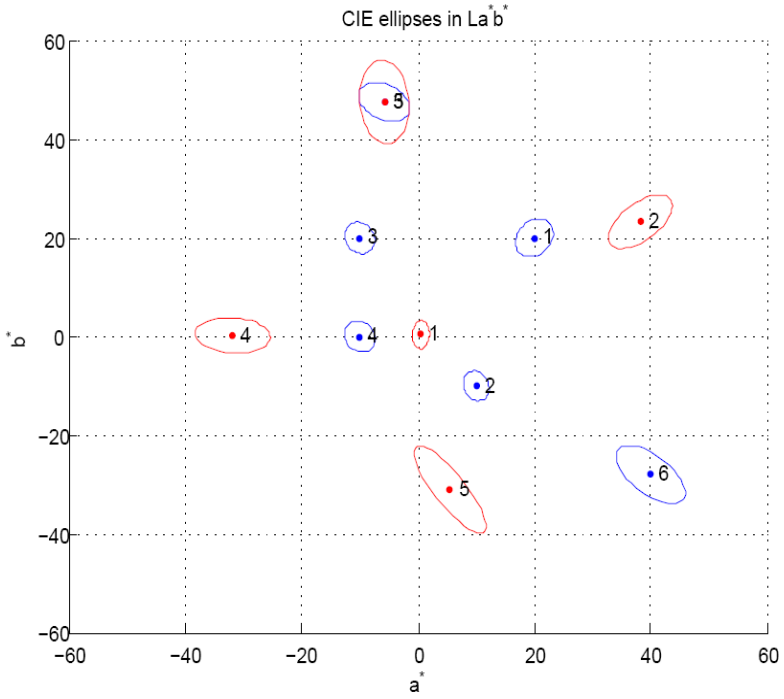

Figure 17. CIE chromaticity ellipses (red set) and new ellipses in the a^*b^* diagram (blue set).

6.3.2 Experimental results of color density g_{comb} values

Figure 18 and 19 show the computed color densities, g_{comb} values, throughout the entire xy chromaticity diagram.

The color density values in the xyY and CIELAB color spaces are 4-dementional data sets, thus the visualization of color density values becomes more complicated. However, the isosufaces could be used to visualize the color density. Figure 20 shows the isosurfaces of color densities in the xyY color space. As can be seen from Figure 20, five isosurfaces with different colors are plotted, and the isovalues for the isosurfaces from the bottom to the top are 0.25, 0.5, 2.0, 5.0 and 8.0, respectively.

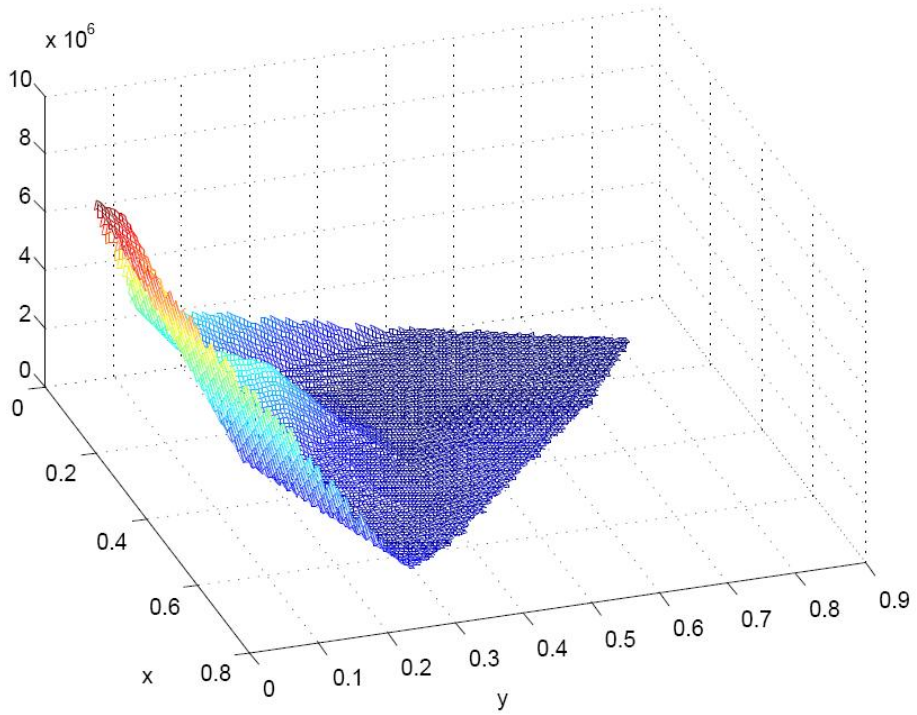

Figure 18. Surface of color densities (g_{comb}) over xy diagram.

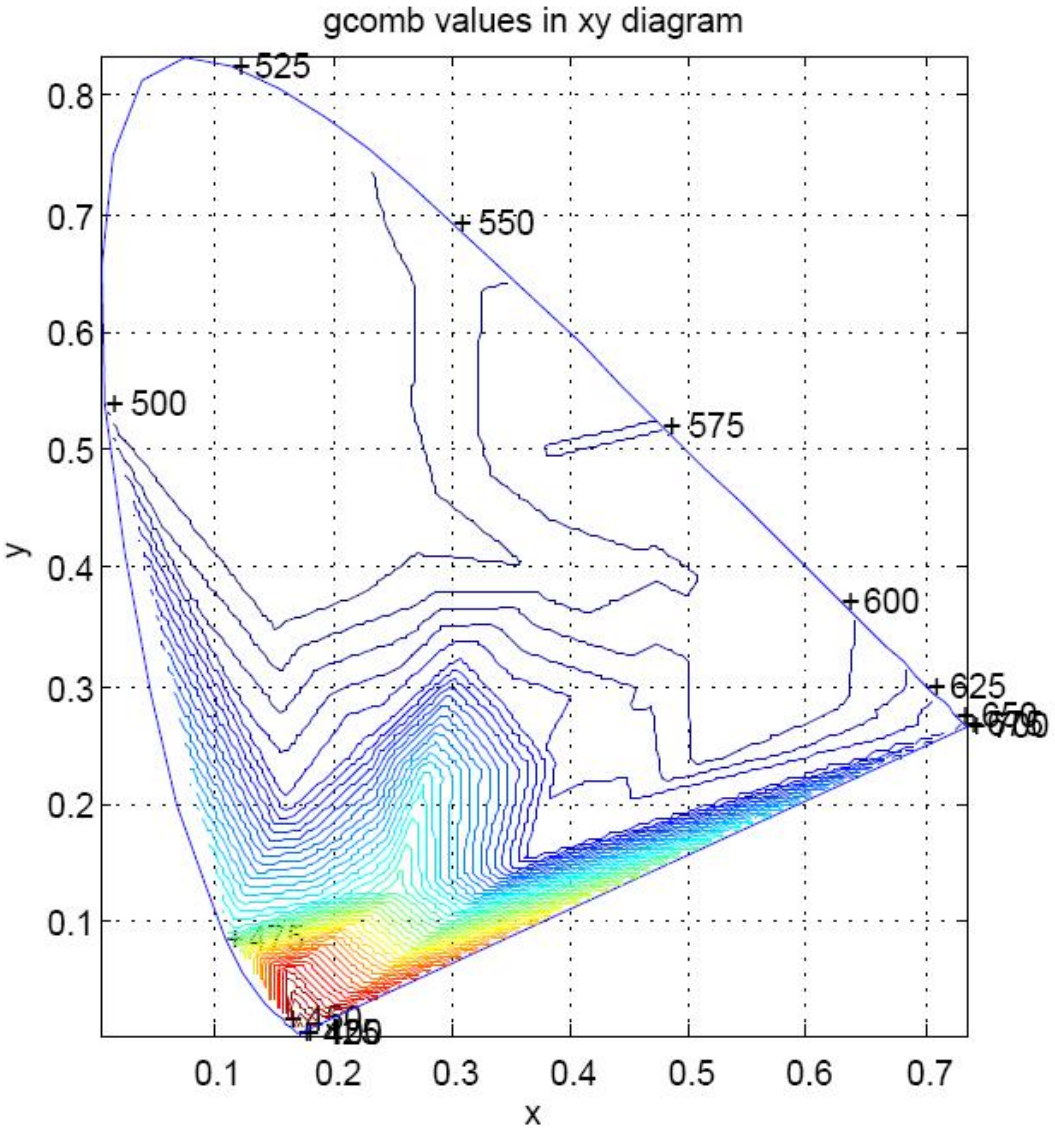

Figure 19. Contours of color densities (g_{comb}) over the *xy* diagram.

Furthermore, Figure 21 shows the cyan and red surfaces in Figure 20 in a more clear view position.

Figure 22 illustrates the isosurfaces of color densities in CIELAB color space. In Figure 22, three isosurfaces at isovalues of 2.0, 1.2 and 0.5 are plotted on the a*b* diagram in blue, green and red.

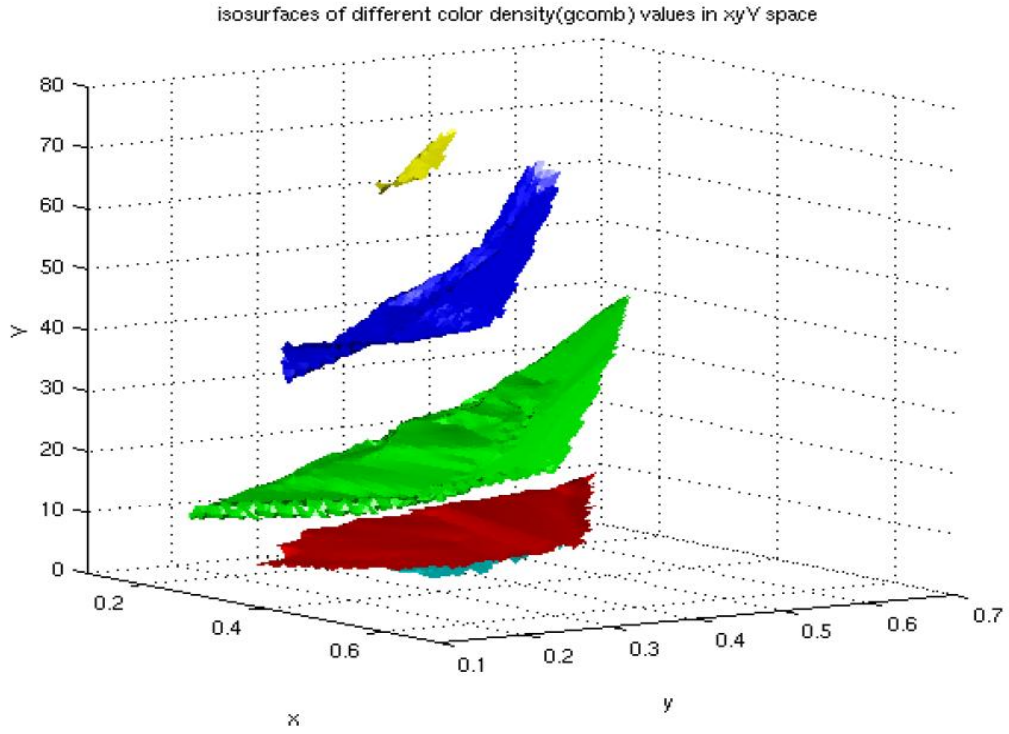

Figure 20. The isosurfaces of color densities in the *xyY* color space. The isovalues are 0.25, 0.5, 2.0, 5.0 and 8.0 for surfaces from bottom to top.

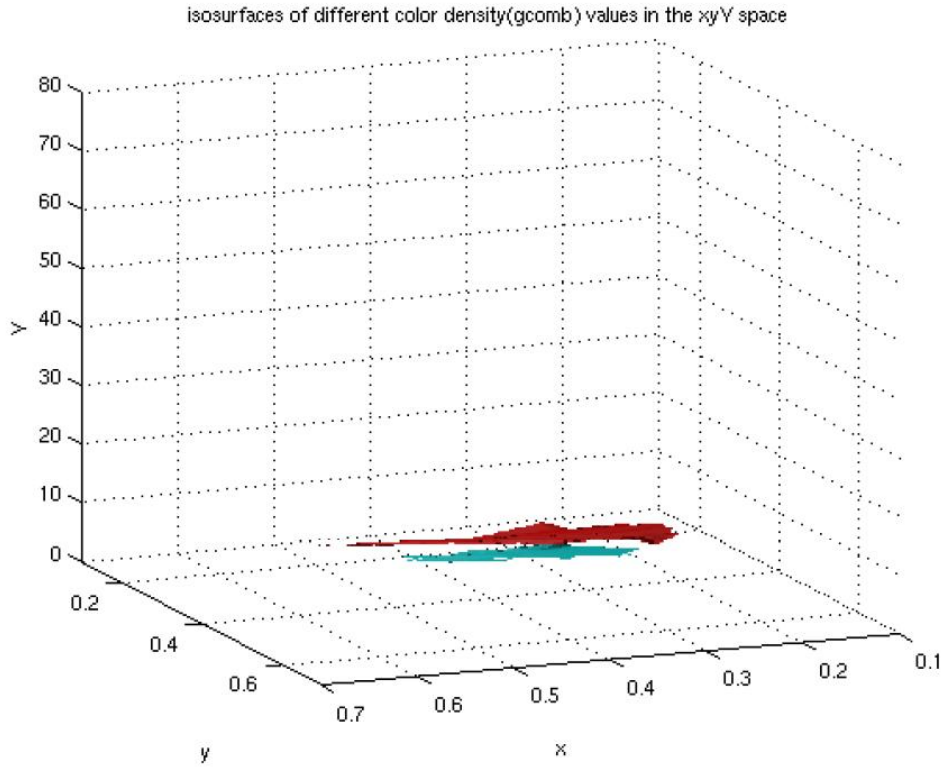

Figure 21. The isosurfaces at isovalues 0.25 and 0.5 from bottom to top.

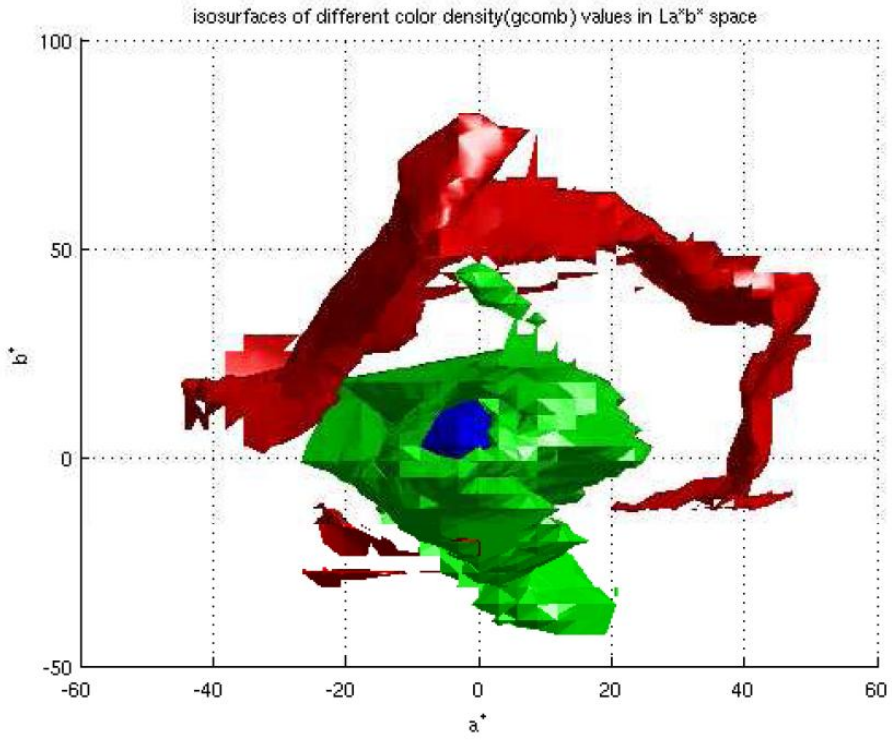

Figure 22. The isosurfaces of color density plotted in the a*b* diagram. The isovalues are 2.0, 1.2 and 0.5 for blue, green and red surfaces.

6.3.3 Experimental results of chromaticity differences

MacAdam ellipses 1#, 12#, 16#, 7# and 4# were located in different color areas in the xy diagram. Therefore these five MacAdam ellipses were selected for testing the results calculated by different chromaticity difference formulas. Two pairs of chromaticity points were made for each ellipse: both the pairs started from the ellipse center point, one end point was in the direction of the ellipse major semi-axis a, and the other one was in the direction of the minor semi-axis b. Tables 5-7 collected the results calculated by Eqs. 49-51 for Experiments 1-3, respectively. Furthermore, Tables 8-10 showed the density based chromaticity differences from Eqs. 52-53 for the three experimental settings.

In the xyY and CIELAB color spaces, the same pairs of chromaticity points as in the xy diagram were fixed for five CIE discrimination ellipses. The five CIE

discrimination ellipses were recommended for color difference evaluations [29]. Tables 11-13 collected the results of Eqs. 49-51 in the xyY space for Experiments 1-3, and Table 14-16 showed the density based chromaticity differences from Eqs.52-53 for the three experimental settings. Tables 17-19, and 20-22 collected the results computed in CIELAB. In particular, the color differences also were computed by the CIE2000, CIE94 and CMC color differences formulas, and the results were shown in Tables 23-25.

Table 5. Computed chromaticity differences results for Experiment 1 in the xy diagram. ω=0 indicates the end point on major semi-axis a and $\omega = pi/2$ indicates the end point on minor semi-axis b.

Ellipse	dis		$ds1$		$ds2$	
	ω=0	$\omega = pi/2$	ω=0	$\omega = pi/2$	ω=0	$\omega = pi/2$
$1^{\#}$	0.0008	0.0003	1.0000	1.0000	0.9977	0.9985
$12^{\#}$	0.0031	0.0009	1.0000	1.0000	0.9982	0.9984
$16^{\#}$	0.0026	0.0013	1.0000	1.0000	0.9985	0.9980
$7^{\#}$	0.0050	0.0020	1.0000	1.0000	1.0074	0.9998
$4^{\#}$	0.0096	0.0023	1.0000	1.0000	1.0434	1.0002

Table 6. Computed chromaticity differences results for Experiment 2 in the xy diagram. ω=0 indicates the end point on major semi-axis a and $\omega = pi/2$ indicates the end point on minor semi-axis b.

Ellipse	dis		$ds1$		$ds2$	
	ω=0	$\omega = pi/2$	ω=0	$\omega = pi/2$	ω=0	$\omega = pi/2$
$1^{\#}$	0.0008	0.0008	1.0000	2.4286	0.9977	2.4196
$12^{\#}$	0.0031	0.0031	1.0000	4.1739	0.9982	3.4257
$16^{\#}$	0.0026	0.0026	1.0000	2.5000	0.9985	1.9920
$7^{\#}$	0.0050	0.0050	1.0000	3.4440	1.0074	2.4990
$4^{\#}$	0.0096	0.0096	1.0000	2.0000	1.0434	4.1779

Table 7. Computed chromaticity differences results for Experiment 3 in the xy diagram. ω=0 indicates the end point on major semi-axis a and $\omega = pi/2$ indicates the end point on minor semi-axis b.

Ellipse	dis		$ds1$		$ds2$	
	ω=0	$\omega = pi/2$	ω=0	$\omega = pi/2$	ω=0	$\omega = pi/2$
$1^{\#}$	0.0034	0.0034	4.0000	9.7145	3.9557	9.5811
$12^{\#}$	0.0034	0.0034	1.0821	3.7539	0.3571	1.4796
$16^{\#}$	0.0034	0.0034	1.3045	2.6092	0.6783	1.6995
$7^{\#}$	0.0034	0.0034	0.6800	1.7000	1.0821	3.7539
$4^{\#}$	0.0034	0.0034	0.3542	1.4783	1.3045	2.6092

Table 8. Density based chromaticity differences results for Experiment 1 in the xy diagram. ω=0 indicates the end point on major semi-axis a and $\omega = pi/2$ indicates the end point on minor semi-axis b.

Ellipse	$g_{comb}/10^6$	$ds3$		$ds4\_1$		$ds4\_2*10^3$	
		ω=0	$\omega = pi/2$	ω=0	$\omega = pi/2$	ω=0	$\omega = pi/2$
$1^{\#}$	7.5668	5.8741	0.1704	2.3336	0.9612	6.4063	2.6384
$12^{\#}$	0.3610	11. 7764	0.0836	3.3645	0.9786	2.1166	0.9250
$16^{\#}$	1.1860	3.9984	0.2514	1.8987	0.9484	1.4914	0.6571
$7^{\#}$	0.2326	6.2813	0.1593	2.4184	0.9645	1.1681	0.4648
$4^{\#}$	0.1839	17.3649	0.0566	4.1064	0.9870	1.7536	0.4229

Table 9. Density based chromaticity differences results for Experiment 2 in the xy diagram. ω=0 indicates the end point on major semi-axis a and $\omega = pi/2$ indicates the end point on minor semi-axis b.

Ellipse	$g_{comb}/10^6$	$ds3$		$ds4\_1$		$ds4\_2*10^3$	
		ω=0	$\omega = pi/2$	ω=0	$\omega = pi/2$	ω=0	$\omega = pi/2$
$1^{\#}$	7.5668	2.4237	1.0060	2.3336	2.3287	6.4063	6.3728
$12^{\#}$	0.3610	3.4317	0.9864	3.3645	3.3577	3.6495	3.6295
$16^{\#}$	1.1860	1.9996	1.0005	1.8987	1.8945	1.3886	1.3741
$7^{\#}$	0.2326	2.5062	0.9864	2.4184	2.4112	1.1681	1.1606
$4^{\#}$	0.1839	4.1871	0.9766	4.1064	4.1299	1.7536	1.7658

Table 10. Density based chromaticity differences results for Experiment 3 in the xy diagram. ω=0 indicates the end point on major semi-axis a and $\omega = pi/2$ indicates the end point on minor semi-axis b.

Ellipse	$g_{comb}/10^6$	$ds3$		$ds4\_1$		$ds4\_2*10^4$	
		ω=0	$\omega = pi/2$	ω=0	$\omega = pi/2$	ω=0	$\omega = pi/2$
$1^{\#}$	7.5668	9.6357	4.1090	7.0540	6.9904	2.5321	2.4791
$12^{\#}$	0.3610	3.7624	1.0805	2.8030	2.7967	0.4000	0.3876
$16^{\#}$	1.1860	2.6146	1.3171	1.8865	1.8809	0.1817	0.1792
$7^{\#}$	0.2326	2.5062	1.7029	1.2484	1.2459	0.0793	0.0790
$4^{\#}$	0.1839	1.4774	0.3507	1.1064	1.1090	0.0624	0.0625

Table 11. Computed chromaticity differences results for Experiment 1 in the *xyY* space. ω=0 indicates the end point on major semi-axis a and $\omega = pi/2$ indicates the end point on minor semi-axis b.

Ellipse	*dis*		$ds1*10^3$		$ds2*10^3$	
	ω=0	$\omega = pi/2$	ω=0	$\omega = pi/2$	ω=0	$\omega = pi/2$
$1^{\#}$	0.0036	0.0011	0.1323	0.1862	0.1332	0.1862
$12^{\#}$	0.0109	0.0032	0.6971	0.3493	0.7933	0.3568
$16^{\#}$	0.0070	0.0030	0.4929	0.6435	0.1164	0.7118
$7^{\#}$	0.0060	0.0054	0.7197	0.4442	0.7317	0.4617
$4^{\#}$	0.0161	0.0027	0.6239	0.2896	0.6158	0.2891

Table 12. Computed chromaticity differences results for experiment 2 in the *xyY* space. ω=0 indicates the end point on major semi-axis a and $\omega = pi/2$ indicates the end point on minor semi-axis b.

Ellipse	*dis*		$ds1*10^3$		$ds2*10^3$	
	ω=0	$\omega = pi/2$	ω=0	$\omega = pi/2$	ω=0	$\omega = pi/2$
$1^{\#}$	0.0036	0.0036	0.1323	0.5904	0.1339	0.5907
$12^{\#}$	0.0109	0.0109	0.6971	1.1877	0.7884	1.2159
$16^{\#}$	0.0070	0.0070	0.4929	1.4864	0.1725	0.1694
$7^{\#}$	0.0060	0.0060	0.7197	0.4931	0.7320	0.5130
$4^{\#}$	0.0161	0.0161	0.6239	1.7378	0.5981	1.7284

Table 13. Computed chromaticity differences results for Experiment 3 in the xyY space. ω=0 indicates the end point on major semi-axis a and $\omega = pi/2$ indicates the end point on minor semi-axis b.

Ellipse	dis		$ds1*10^3$		$ds2*10^3$	
	ω=0	$\omega = pi/2$	ω=0	$\omega = pi/2$	ω=0	$\omega = pi/2$
$1^{\#}$	0.0087	0.0087	0.9681	1.0957	0.9622	1.0917
$12^{\#}$	0.0087	0.0087	0.4913	0.9833	0.5890	0.9943
$16^{\#}$	0.0087	0.0087	1.2291	1.5092	1.2112	1.5769
$7^{\#}$	0.0087	0.0087	1.0654	0.6819	1.0609	0.6819
$4^{\#}$	0.0087	0.0087	0.9584	0.2775	0.9584	0.2775

Table 14. Density based chromaticity differences results for Experiment 1 in the xyY space. ω=0 indicates the end point on major semi-axis a and $\omega = pi/2$ indicates the end point on minor semi-axis b.

Ellipse	$g_{comb}*10$	$ds3*10^3$		$ds4\_1*10^3$		$ds4\_2*10^8$	
		ω=0	$\omega = pi/2$	ω=0	$\omega = pi/2$	ω=0	$\omega = pi/2$
$1^{\#}$	8.3325	0.5973	0.0893	0.5740	0.1811	0.9151	0.2887
$2^{\#}$	4.8192	1.5961	0.2511	1.5168	0.4461	2.1107	0.6208
$3^{\#}$	9.9647	1.3415	0.2692	1.2878	0.5575	2.3692	1.0256
$4^{\#}$	2.1965	0.9331	0.4180	0.8934	0.8049	1.3303	1.1985
$5^{\#}$	2.5184	0.4180	0.2032	2.1924	0.3654	2.9854	0.4976

Table 15. Density based chromaticity differences results for Experiment 2 in the xyY space. ω =0 indicates the end point on major semi-axis a and $\omega = pi/2$ indicates the end point on minor semi-axis b.

Ellipse	g_{comb}	$ds3*10^3$		$ds4\_1*10^3$		$ds4\_2*10^8$	
		ω =0	$\omega = pi/2$	ω =0	$\omega = pi/2$	ω =0	$\omega = pi/2$
$1^{\#}$	3.8284	0.5973	0.2832	0.5740	0.5740	0.9151	0.9151
$2^{\#}$	0.6657	1.5961	0.8537	1.5168	1.5168	2.1107	2.1107
$3^{\#}$	0.4574	1.3415	0.6220	1.2878	1.2878	2.3692	2.3692
$4^{\#}$	0.6201	0.9331	0.4640	0.8934	0.8934	1.3303	1.3303
$5^{\#}$	1.0654	2.3016	1.2192	2.1924	2.1924	2.9854	2.9854

Table 16. Density based chromaticity differences results for Experiment 3 in the xyY space. ω =0 indicates the end point on major semi-axis a and $\omega = pi/2$ indicates the end point on minor semi-axis b.

Ellipse	g_{comb}	$ds3*10^3$		$ds4\_1*10^3$		$ds4\_2*10^8$	
		ω =0	$\omega = pi/2$	ω =0	$\omega = pi/2$	ω =0	$\omega = pi/2$
$1^{\#}$	3.8284	1.4435	0.6843	1.3871	1.3871	2.2116	2.2116
$2^{\#}$	0.6657	1.2739	0.6841	1.2107	1.2107	1.6847	1.6847
$3^{\#}$	0.4574	1.6672	0.7730	1.6006	1.6006	2.9446	2.9446
$4^{\#}$	0.6201	1.3529	0.6728	1.2954	1.2954	1.9289	1.9289
$5^{\#}$	1.0654	1.2437	0.6588	1.1847	1.1847	1.6132	1.6132

Table 17. Computed chromaticity differences results for Experiment 1 in the CIELAB space. ω=0 indicates the end point on major semi-axis a and $\omega = pi/2$ indicates the end point on minor semi-axis b.

Ellipse	*dis*		*ds*1		*ds*2	
	ω=0	$\omega = pi/2$	ω=0	$\omega = pi/2$	ω=0	$\omega = pi/2$
1#	0.9521	0.4846	1.0000	1.0000	1.0092	0.9251
2#	2.2898	1.1623	1.0001	1.0000	0.9736	0.9414
3#	2.8295	1.4046	1.0000	1.0000	1.0000	1.0000
4#	2.1473	1.1957	1.0001	1.0000	1.0399	1.0003
5#	3.4655	0.9515	0.9999	1.0000	1.5757	0.9984

Table 18. Computed chromaticity differences results for Experiment 2 in the CIELAB space. ω=0 indicates the end point on major semi-axis a and $\omega = pi/2$ indicates the end point on minor semi-axis b.

Ellipse	*dis*		*ds*1		*ds*2	
	ω=0	$\omega = pi/2$	ω=0	$\omega = pi/2$	ω=0	$\omega = pi/2$
1#	0.9521	0.9521	1.0000	1.9648	1.0092	1.7286
2#	2.2898	2.2898	1.0001	1.9701	0.9736	1.8477
3#	2.8295	2.8295	1.0000	2.0145	1.0000	2.0656
4#	2.1473	2.1473	1.0001	1.7958	1.0399	1.7967
5#	3.4655	3.4655	0.9999	3.6421	1.5757	3.6209

Table 19. Computed chromaticity differences results for Experiment 3 in the CIELAB space. ω=0 indicates the end point on major semi-axis a and $\omega = pi/2$ indicates the end point on minor semi-axis b.

Ellipse	*dis*		*ds*1		*ds*2	
	ω=0	$\omega = pi/2$	ω=0	$\omega = pi/2$	ω=0	$\omega = pi/2$
1#	2.2800	2.2800	2.3947	4.7052	2.4471	4.0532
2#	2.2800	2.2800	0.9958	1.9617	0.9958	1.8398
3#	2.2800	2.2800	0.8058	1.6233	0.8058	1.6645
4#	2.2800	2.2800	1.0619	1.9068	1.1067	1.9078
5#	2.2800	2.2800	0.6579	2.3962	1.0069	2.3870

Table 20. Density based chromaticity differences results for Experiment 1 in the CIELAB space. ω=0 indicates the end point on major semi-axis a and $\omega = pi/2$ indicates the end point on minor semi-axis b.

Ellipse	g_{comb}	*ds*3		*ds*4_1		*ds*4_2	
		ω=0	$\omega = pi/2$	ω=0	$\omega = pi/2$	ω=0	$\omega = pi/2$
1#	3.8284	1.8584	0.5333	1.7543	0.8739	3.2325	1.5760
2#	0.6657	1.9570	0.7000	1.8588	0.9161	1.5089	0.7221
3#	0.4574	2.0145	0.4964	1.9137	0.9500	1.2943	0.6425
4#	0.6201	1.7926	0.5679	1.6833	0.9405	1.3195	0.7398
5#	1.0654	4.2082	0.2906	4.0823	1.0063	4.8090	1.0063

Table 21. Density based chromaticity differences results for Experiment 2 in the CIELAB space. ω=0 indicates the end point on major semi-axis a and $\omega = pi/2$ indicates the end point on minor semi-axis b.

Ellipse	g_{comb}	$ds3$		$ds4\_1$		$ds4\_2$	
		ω=0	$\omega = pi/2$	ω=0	$\omega = pi/2$	ω=0	$\omega = pi/2$
$1^{\#}$	3.8284	1.8584	1.0471	1.7543	1.6507	3.2325	2.8619
$2^{\#}$	0.6657	1.9570	1.3752	1.8588	1.8003	1.5089	1.4154
$3^{\#}$	0.4574	2.0145	0.9471	1.9137	1.9758	1.2943	1.3797
$4^{\#}$	0.6201	1.7926	1.0354	1.6833	1.6878	1.3195	1.3266
$5^{\#}$	1.0654	4.2082	1.1953	4.0823	3.5325	4.8090	3.6008

Table 22. Density based chromaticity differences results for Experiment 3 in the CIELAB space. ω=0 indicates the end point on major semi-axis a and $\omega = pi/2$ indicates the end point on minor semi-axis b.

Ellipse	g_{comb}	$ds3$		$ds4\_1$		$ds4\_2$	
		ω=0	$\omega = pi/2$	ω=0	$\omega = pi/2$	ω=0	$\omega = pi/2$
$1^{\#}$	3.8284	4.1092	2.4200	3.8719	3.8738	6.5754	6.5819
$2^{\#}$	0.6657	1.9486	1.3694	1.8509	1.7926	1.5025	1.4095
$3^{\#}$	0.4574	1.6233	0.7631	1.5420	1.5921	1.0429	1.1118
$4^{\#}$	0.6201	1.9032	1.1017	1.7869	1.7919	1.4004	1.4083
$5^{\#}$	1.0654	2.8575	0.7459	2.7876	0.7459	3.4082	2.3334

Table 23. Results of the color differences formulas for Experiment 1 in the CIELAB space. ω=0 indicates the end point on major semi-axis a and $\omega = pi/2$ indicates the end point on minor semi-axis b.

Ellipse	L	CIEDE2000		CIE94		CMC	
		ω=0	$\omega = pi/2$	ω=0	$\omega = pi/2$	ω=0	$\omega = pi/2$
1#	61.3164	0.9215	0.7171	62.4817	62.4825	41.4360	41.4442
2#	44.8012	0.8038	0.7476	48.4101	42.9493	37.7785	33.7064
3#	86.9429	0.8834	0.9389	211.2434	212.2714	117.229	117.633
4#	56.2576	0.8790	0.8041	154.2998	152.4796	90.0257	88.1982
5#	35.8685	0.9178	0.8651	68.5071	69.7481	40.2929	41.0344

Table 24. Results of the color differences formulas for Experiment 2 in the CIELAB space. ω=0 indicates the end point on major semi-axis a and $\omega = pi/2$ indicates the end point on minor semi-axis b.

Ellipse	L	CIEDE2000		CIE94		CMC	
		ω=0	$\omega = pi/2$	ω=0	$\omega = pi/2$	ω=0	$\omega = pi/2$
1#	61.3164	0.9215	1.4174	62.4817	62.4870	41.4360	41.4543
2#	44.8012	0.8038	1.4822	48.4101	42.2047	37.7785	32.4072
3#	86.9429	0.8834	1.8793	211.2434	212.5303	117.229	118.15
4#	56.2576	0.8790	1.4454	154.2998	152.5360	90.0257	88.2550
5#	35.8685	0.9178	3.0919	68.5071	67.3760	40.2929	39.6241

Table 25. Results of the color differences formulas for Experiment 3 in the CIELAB space. ω=0 indicates the end point on major semi-axis a and $\omega = pi/2$ indicates the end point on minor semi-axis b.

Ellipse	L	CIEDE2000		CIE94		CMC	
		ω=0	$\omega = pi/2$	ω=0	$\omega = pi/2$	ω=0	$\omega = pi/2$
1#	61.3164	2.1471	3.2993	62.4819	62.5310	41.4355	41.4967
2#	44.8012	0.8005	1.4758	48.3944	41.2198	37.7668	32.4184
3#	86.9429	0.7146	1.5182	211.2117	213.0388	117.218	117.948
4#	56.2576	0.9320	1.5349	154.4204	152.5439	90.1466	88.2629
5#	35.8685	0.5889	2.0533	62.2387	68.4833	40.7290	40.2788

7 DISCUSSION

In the xy chromaticity diagram, the interpolation results of metric coefficients g_{ik} for chromaticity colors were shown in the form of discrimination ellipses and line element $ds2$. These discrimination ellipses presented nearly the same variation trend as the original MacAdam ellipses both in sizes and in orientations. In the three experiments, the results of $ds2$ which were calculated from the interpolated g_{ik} approximated to the line element $ds1$ of original data very well.

The color density g_{comb} reached the maximum for the ellipse in blue area. However, the minimum color density g_{comb} occurred in green area. Furthermore, the intermediate color densities were in the area between blue and green, and they became larger from the bottom area to the top area. This indicated the same variation trend as the ellipse size changed. In Experiments 2 and 3, the chromaticity differences from the ellipse center along the ellipses major semi-axis a were always smaller than along the minor semi-axis b, which occurred both inside and outside ellipses. However, the chromaticity differences calculated from $ds3$ did not obey this rule.

The chromaticity differences calculated by $ds4\_1$ and $ds4\_2$ are nearly constant for each circle in Experiments 2 and 3. Especially in Experiment 3, the larger color density a color had, the larger chromaticity differences have been estimated. As compared to $ds4\_2$, $ds4\_1$ computed chromaticity difference with relative small magnitude, and they are more approximate to the color differences computed by $ds1$.

In the xyY color space, the results were calculated by $ds1$ and $ds2$ based on the recalculated g_{ik}, and these results predicted the perceived chromaticity differences with significant magnitudes which were not close to a constant for all ellipses. In addition, they did not consistently prove that the chromaticity differences along the major semi-axis a should be smaller than along the minor semi-axis b in Experiments 2 and 3. However, the chromaticity differences calculated by $ds4\_1$

and $ds4\_2$ showed some trends: the color density increased while the illumination increased, and the corresponding larger chromaticity differences were found. The isosufaces illustrated in Figure 20 also indicated that the blue area (around x=0.2, y=0.2) under lower illumination levels and the green area (around x=0.2, y=0.7) under higher illumination levels have the same color density.

In the CIELAB color space, the results calculated by $ds1$ and $ds2$ were close to each other except for the blue center. For the blue ellipses (a*=5.0, b*=-31.0), the chromaticity differences ($ds2$) along the major semi-axis were always larger than the chromaticity differences ($ds1$) along the same direction. This indicated the interpolation in blue area might be inaccurate. As can be seen from Figure 7 in chapter 4, the data samples in blue area are rare, and neighboring ellipses were larger in the major semi-axis directions, which might cause the interpolated g_{ik} values become larger. However, the chromaticity differences $ds1$ and $ds2$ in Experiments 2 and 3 supported the facts that the chromaticity differences along the major semi-axis a should be smaller than along the minor semi-axis b. In addition, the neutral colors had the largest color density; the larger distances from the neutral center the smaller color density occurred, and the corresponding smaller color differences were found. This trend agreed well with the ellipse size variations of the CIEDE00 ellipse set used in this work. However, compared to the color differences calculated by the CIEDE2000 formula, it is hard to make a conclusion that which density based chromaticity difference performs better than another one in general.

8 CONCLUSIONS

In this work the color density was developed as a quantitative attribute for a color which could be used for estimating the color differences from this color, and color density based chromaticity difference formulas were proposed and tested as well. The color density was derived from the metric coefficients g_{ik} of each color. Since the metric coefficients g_{ik} could be used for constructing the color discrimination ellipses which represented the human perceived color differences from the ellipse center color, the ellipse parameters could be used for computing the metric coefficients g_{ik} as well. The g_{ik} values were combined both in the major semi-axis and in the minor semi-axis directions to a single value for the ellipses center color. However, in order to find the color densities for the colors which were not the ellipse center colors, interpolation methods should be used.

The color density achieved revealed the variation trends of discrimination ellipses in the xy chromaticity diagram and in the CIELAB color space, which agreed well with MacAdam ellipses and the CIEDE00 ellipse set. Furthermore, the dependence between color density and illumination levels in the xyY color space found in this work was consistent with the results from Melgosa et al. [30] showing the influence of luminance on the size of discrimination ellipses.

Generally speaking, the color with larger color density yields larger perceived color differences. However, the experimental results also showed some shortcomings for color density: it is not adequate in evaluating the color differences from a color in different directions. Thus, a color could be characterized by the color density which estimates the roughly perceived color differences from this color.

Three color density based chromaticity difference formulas were proposed. Although they provided relatively simple ways to estimate color differences, none of them performed better than the original line element formula or the CIEDE2000 color difference formula. These shortcomings might be caused by: the original line element

formula estimates the color differences by three metric coefficients, and the CIEDE2000 formula contains the directional information which are calculated by the hue angles between colors. However, the metric coefficients $g_{\min}$, $g_{\max}$ and g_{comb} could not provide adequate directional information in estimating color differences.

The future research could focus on improving interpolation methods and discrimination data sets. Also the suitable color density based chromaticity difference formulas would be a part of the future work.

REFERENCES

[1] Luo M.R.. Color difference formulae: past, present and future. Available at: http://www.iscc.org/jubilee2006/abstracts/LuoAbstract.pdf. Access on: 27/4/2009.

[2] Kuehni Rolf G.. Color difference formulas: an unsatisfactory state of affairs. Color Research and Application 2008. 33: 324 -326.

[3] Wyszecki G., Stiles W.S.. Color Science Concept and Methods, Quantitative Data and Formulae, 2nd Ed.. JOHN WILEY & SONS, INC, 2000.

[4] Fairchild Mark D.. Color Appearance Models, 2nd Ed.. JOHN WILEY & SONS, Ltd, 2006.

[5] Wikipedia. Sagitta2. Available at: http://en.wikipedia.org/wiki/File:Human_eye_cross-sectional_view_grayscale.png. Accessed on 15/4/2009.

[6] Wikipedia. Rod cone cells. Available at: http://en.wikipedia.org/wiki/File:Rod_cone_cells.jpg. Accessed on 15/4/2009.

[7] Wikipedia. Cones_SMJ2_E. Available at: http://en.wikipedia.org/wiki/File:Cones_SMJ2_E.svg. Accessed on 15/4/2009.

[8] Kuehni R.G.. Color space and its divisions. Color Research and Application 2001. 26: 209-222.

[9] Billmeyer F. W. J.. Survey of color order systems. Color Research and Application 1987. 12: 173-186.

[10] Burns S. A., Cohen J. B., Kuznetsov E. N.. The Munsell color system in fundamental color space. Color Research and Application 1990. 15: 29-51.

[11] NCS. Available at: http://www.ncscolour.com/webbizz/mainPage/main.asp. Accessed on 13/4/2009.

[12] Ramanath R., Snyder W. E., Kuehni R. G., Hinks D.. Spectral spaces and color spaces. Color Research and Application 2004. 29: 29-37.

[13] Billmeyer F. W. J., Bencuya A. K.. Interrelation of the Natural Color System and the Munsell Color Order System., Color Research and Application 1987. 22:243-255.

[14] Nayatani Yoshinobu. Transformation from munsell space to Swedish NCS-Through Nayatani theoretical space. Color Research and Application 2004. 29: 151-157.

[15] Vos J.J.. Line elements and physiological models of color vision. Color Research and Application 1979, 4: 208-216.

[16] MacAdam D.L.. Visual sensitive to color differences in daylight. Journal of the Optical of American A 1942, 32: 247-274.

[17] MacAdam, David L.. Specification of Small Chromaticity Differences. Journal of the Optical Society of American 1943, 33: 27-30.

[18] Luo M.R., Rigg B.. Chromaticity-discrimination ellipses for surface colors. Color Research and Application 1986, 11: 25-42.

[19] Luo M.R., Cui G., Rigg B.. The development of the CIE2000 color-difference formula: CIEDE2000. Color Research and Application 2001, 26: 340-350.

[20] Robertson, A.R.. Historical Development of CIE Recommended Color Difference Equations. Color Research and Application 1990, 15: 167-170.

[21] Color Research and Application. CMC Color-Difference Formula. Color Research and Application 1984, 9, 250.

[22] Melgosa M. Testing CIELAB-based color-difference formulas. Color Research and Application 2000. 25: 49-55.

[23] Imai F.H., Tsumura N., Miyake Y.. Perceptual color difference metric for c omplex images based on Mahalanobis distance. Available at: http://www.mi .tj.chiba-u.jp/~tsumura/Tsumura/papers/JEIManuscriptFinal_mahalanobis.pdf. A ccess on:27/4/2009.

[24] Melgosa M., Hita E., Poza A.J., Perez M.M.. The Weighting Function for Lightness in the CIE94 Color-Difference Model. Color Research and Application 1996, 21: 347-352.

[25] Kuehni R.G.. Analysis of five sets of color difference data. Color Research and Application 2001, 26: 141-150.

[26] Melgosa M. Color-difference Formula. Available at: http://www.balkanlight.e u/abstracts_pdf/i24.pdf. Access on: 27/4/2009.

[27] Wikipedia. Von Mises yield criterion. Available at: http://www.en.wikipedia.org/wiki/Von_Mises_yield_criterion. Access on: 15/9/2009.

[28] MacAdam, David L., Metric Coefficients for CIE Color-Difference Formulas. Color Research and Application 1985, 10: 45-49.

[29] Robertson, A. R., CIE guidelines for coordinated research on colour-difference evaluation, Color Research and Application 1978, 3: 149-151.

[30] Melgosa, M., Perez M. M., Moraghi, A. EI, Hita E., Color Discrimination Results form a CRT Device: Influence of Luminance. Color Research and Application 1999, 24: 38-44.